

Solvent Reorganization Energy and Entropy in Hydrophobic Hydration

Themis Lazaridis*

Department of Chemistry, City College of CUNY, Convent Ave & 138th Street, New York, New York 10031

Received: December 6, 1999; In Final Form: March 20, 2000

Monte Carlo simulations of methane in water at 25, 65, and 160 °C are used to obtain the water binding energy as a function of distance from the solute, average water pair interaction energies in the first and second solvation shell, the triplet solute–water oxygen–water oxygen correlation function, the water orientational distribution with respect to the solute as a function of distance from the solute, and water–water orientational correlation functions in the first and second solvation shells. The calculated correlation functions are used in conjunction with the inhomogeneous forms of the energy equation and the correlation expansion for the entropy [Lazaridis, *J. Phys. Chem.* **1998**, 102, 3531] to calculate the solvent reorganization energy and entropy. It is shown that these quantities contain two large contributions of opposite sign: a positive contribution from the exclusion of solvent molecules by the solute and a negative contribution from the orientational arrangement of water next to the solute. The large magnitude of the heat capacity of hydration is due to flattening of the water orientational distribution with respect to the solute as the temperature increases, which leads to diminution of the orientational arrangement contribution and concomitant increase in both the enthalpy and the entropy of solvation.

I. Introduction

The hydration of small nonpolar molecules (hydrophobic hydration) at room temperature is characterized by a positive free energy, a negative enthalpy, a negative entropy that dominates over the enthalpy, and a large positive heat capacity. Due to the last, the solvation enthalpy and entropy become less negative and eventually positive at higher temperatures, with the enthalpic term becoming progressively more important as the temperature increases. The goal of any molecular theory of solvation is to account for these macroscopic thermodynamic properties in terms of microscopic interactions and the structure of water around nonpolar solutes.

Several theoretical methods have been applied to hydrophobic hydration. Pratt and Chandler¹ were the first to employ a rigorous liquid state theory to study this problem. They developed a perturbation theory treatment with the hard sphere fluid as a reference state. Matching the experimental solubility at room temperature and using the experimental temperature-dependent density of water, they developed a description of the thermodynamic properties of hydrophobic solvation. Moreover, a Percus–Yevick-like integral equation approach using the experimental water radial distribution functions provided reasonable correlation functions between two hydrophobic solutes in water. The extended reference interaction site model (X-RISM) integral equation approach was also applied to hydrophobic solvation, but it was found that the hypernetted chain closure inherent in this theory predicts solvation free energies for hydrophobic groups that are too positive.^{2–4} The more recent information theory model^{5,6} offers a prescription for calculating the probability of observing a cavity of arbitrary size and shape (and therefore the chemical potential of a hard solute of the same size and shape) using the experimental density and radial distribution function of water. Although these theoretical

approaches are very useful, they do not provide a connection with the widely accepted intuitive pictures of the hydrophobic effect, such as the concepts of solvent structure making and breaking and clathrate cage formation resulting from the presence of the hydrophobic solute in water. It is one of the purposes of the present work to make this connection based on a correlation function formulation.

Computer simulations have played an important role in increasing our understanding of the structure and energetics of water and aqueous solutions. Simulations of small hydrophobic solutes showed that water adopts a flickering clathrate-like arrangement around nonpolar groups so as to minimize the loss of its hydrogen bonds.^{7–17} Detailed analyses of the interactions of water molecules in the hydration shell of nonpolar solutes (water binding energies and water pair interactions) as well as solute–water and water–water radial distribution functions in the hydration shell have been reported (see, for example, refs 10, 18, 19). Since the interactions used in the simulations are usually pairwise additive, the solvation energy is commonly separated into two contributions: the solute–solvent interaction energy and the change in the solvent–solvent energy upon solute insertion, which is referred to as solvent reorganization energy.^{20–22} Free energy simulations have been applied to calculate the solvation free energy^{23–27} and have obtained positive solvation free energies for hydrophobic solutes in reasonable agreement with experimental values. This indicates that the molecular mechanics potentials used in the simulations do describe the physics of this process. However, the results have not aided significantly in the physical understanding of hydrophobic hydration because they do not reveal the origin of this positive free energy.

Although the free energies can be calculated with reasonable reliability, obtaining accurate values for the enthalpies and entropies from simulations is much more difficult because the statistical fluctuations of the quantities averaged are much larger for the energy and entropy than for the free energy. The entropic

* E-mail: themis@sci.ccny.cuny.edu. Phone: (212) 650-8364. Fax: (212) 650-6107.

term can be obtained, in principle, by subtracting the energy from the free energy or by taking the temperature derivative of the free energy, but very long simulations are required to obtain accurate results.^{25,28,29} More importantly for our present work, even when the results are accurate, they do not reveal the physical origin of the entropy. For example, without more information it is not possible to distinguish between excluded volume entropy and entropy associated with hydrogen bond formation (essentially orientational entropy). One approach that can provide such information is the correlation expansion for the entropy.^{30,31} This expansion gives the entropy as a sum of one-, two-, and higher order terms and is capable of clarifying the origin of solvation entropies. It allows the approximate decomposition of the solvation entropy into solute–solvent and solvent reorganization terms, in analogy with that used for the energy. This approach has been applied to calculate the contribution of solute–solvent correlations to the entropy of hydrophobic solutes in water.^{14,15,32} It has also been used to calculate the contribution of pair correlations to the entropy of liquid water.³³

Recently the correlation expansion treatment was extended to allow the calculation of solvent reorganization energies and entropies using an “inhomogeneous fluid” approach.^{34,35} In this approach, the solute is considered fixed at the origin and creates an inhomogeneous density field around it.³⁶ The solvent reorganization energy and entropy are obtained by taking the difference between the energy and entropy of the solution, viewed as an inhomogeneous system, and the pure solvent. In this paper we employ the formalism to estimate the solvent reorganization energy and entropy of methane in water at 25, 65, and 160 °C. The results, combined with the solute–solvent energy and entropy, provide a detailed molecular interpretation of hydrophobic hydration thermodynamics.

II. Theory

The partial molar energy and entropy of a solute are defined as the derivative of the total energy or entropy with respect to the number of moles of the solute at constant T and P . In statistical thermodynamics they correspond to the change in energy and entropy upon addition of one mole of solute to the solution. The process of addition of a solute can be decomposed into two steps: (a) insertion of the solute at a fixed point, without thermal motion, and (b) imparting thermal motion to the solute (“liberation”).³⁷ The thermodynamic quantities characterizing the first step are Ben-Naim’s proposed standard energy and entropy of solvation. These standard properties are related, but not identical, to the more common excess partial molar properties (excess with respect to an ideal gas at the same temperature and density). The relationship between the two is^{38,34}

$$\bar{e}^{\text{ex}} = \Delta E^* + kT(\alpha - P\kappa) \quad (1)$$

$$\bar{s}^{\text{ex}} = \Delta S^* + k(T\alpha - 1) \quad (2)$$

where α and κ are the thermal expansion coefficient and the isothermal compressibility of the solvent, respectively. For water at room temperature, $T\alpha = 0.077$ and $P\kappa = 45 \times 10^{-6}$, so that $\bar{e}^{\text{ex}} \approx \Delta E^*$ and $\bar{s}^{\text{ex}} \approx \Delta S^* - k$. Similarly, the liberation properties are related, but not identical, to the ideal gas properties at the same temperature and density. The liberation properties at infinite dilution are independent of the nature of the solute and depend only on pure solvent properties.

Explicit expressions for the standard and the liberation energy and entropy in the context of the inhomogeneous fluid approach

have been derived.³⁴ Because the liberation properties for water under ambient conditions are negligible, we are concerned in this work only with Ben-Naim’s standard energy and entropy of solvation. They can be divided into solute–solvent and solvent reorganization terms, that is

$$\Delta E^* = E_{\text{sw}} + \Delta E_{\text{ww}}^{\text{cor}} \quad (3)$$

$$\Delta S^* = S_{\text{sw}}^{\text{ord}} + \Delta S_{\text{ww}}^{\text{cor}} \quad (4)$$

where the subscripts s and w stand for solute and solvent, respectively. The solvent reorganization energy defined by Yu and Karplus²¹ differs from $\Delta E_{\text{ww}}^{\text{cor}}$ in two ways: it includes the “liberation” term and, more importantly from the quantitative viewpoint, refers to solute insertion at constant volume. The solvent reorganization entropy defined here does not correspond to any quantity that appears in the Yu and Karplus analysis. The solvent reorganization energy and entropy defined here tend to compensate but do not completely cancel out.³⁴ These and all of the following equations assume pairwise additivity of the potential energy and consider only two-particle contributions to the correlation function expansion of the entropy. For a given conformation of an infinitely dilute solute in water, the terms in eqs 3 and 4 have the form

$$E_{\text{sw}} = \frac{\rho}{\Omega} \int g_{\text{sw}}(\mathbf{r}, \omega) u_{\text{sw}}(\mathbf{r}, \omega) d\mathbf{r} d\omega \quad (5)$$

$$S_{\text{sw}}^{\text{ord}} = -k \frac{\rho}{\Omega} \int g_{\text{sw}}(\mathbf{r}, \omega) \ln g_{\text{sw}}(\mathbf{r}, \omega) d\mathbf{r} d\omega \quad (6)$$

$$\Delta E_{\text{ww}}^{\text{cor}} = \frac{1}{2} \frac{\rho^2}{\Omega^2} \int g_{\text{sw}}(\mathbf{r}, \omega) [g_{\text{sw}}(\mathbf{r}', \omega') g_{\text{ww}}^{\text{inh}}(\mathbf{r}, \mathbf{r}', \omega, \omega') - g_{\text{ww}}^{\text{o}}(R, \omega^{\text{rel}})] u_{\text{ww}}(R, \omega^{\text{rel}}) d\mathbf{r} d\mathbf{r}' d\omega d\omega' \quad (7)$$

$$\Delta S_{\text{ww}}^{\text{cor}} = -\frac{1}{2} k \frac{\rho^2}{\Omega^2} \times \int g_{\text{sw}}(\mathbf{r}, \omega) [g_{\text{sw}}(\mathbf{r}', \omega') \{g_{\text{ww}}^{\text{inh}} \ln g_{\text{ww}}^{\text{inh}} - g_{\text{ww}}^{\text{inh}} + 1\} - \{g_{\text{ww}}^{\text{o}} \ln g_{\text{ww}}^{\text{o}} - g_{\text{ww}}^{\text{o}} + 1\}] d\mathbf{r} d\mathbf{r}' d\omega d\omega' \quad (8)$$

The functional dependence of $g_{\text{ww}}^{\text{inh}}$ and g_{ww}^{o} in eq 8 is the same as in eq 7. Equations 5–8 are obtained from those in ref 34 which were developed for a monatomic solvent, by addition of orientational degrees of freedom for the solvent. E_{sw} is the solute–solvent energy and $S_{\text{sw}}^{\text{ord}}$ is the “ordering” contribution to the solute–solvent entropy. The latter is the contribution that arises from the fact that the solute–solvent correlation function is not constant, but oscillatory in most cases; the second contribution to the solute–solvent entropy, $\rho f(g - 1) d\mathbf{r}$, accounts for the exclusion of solvent from the volume occupied by the solute. $\Delta E_{\text{ww}}^{\text{cor}}$ and $\Delta S_{\text{ww}}^{\text{cor}}$ are the “correlation” contributions to the solvent reorganization energy and entropy; i.e., the change in solvent–solvent energy and the change in entropy due to solvent–solvent correlations upon insertion of the solute at a fixed point in the solvent. For liquids, where the liberation contributions to the solvent reorganization energy and entropy are negligible, these quantities are close to the total ΔE_{ww} and ΔS_{ww} ($\Delta E_{\text{ww}} = \Delta E_{\text{ww}}^{\text{cor}} + \Delta E_{\text{ww}}^{\text{lib}} \approx \Delta E_{\text{ww}}^{\text{cor}}$, and similarly for ΔS_{ww}).

In eqs 5–8, \mathbf{r} and \mathbf{r}' denote the position of two solvent molecules with respect to the solute, ω and ω' denote the orientation of these solvent molecules with respect to the solute in terms of the three Euler angles, Ω is the integral over ω , ρ is the solvent number density, g_{sw} is the solute–solvent correlation function, g_{ww}^{o} is the pure solvent pair correlation

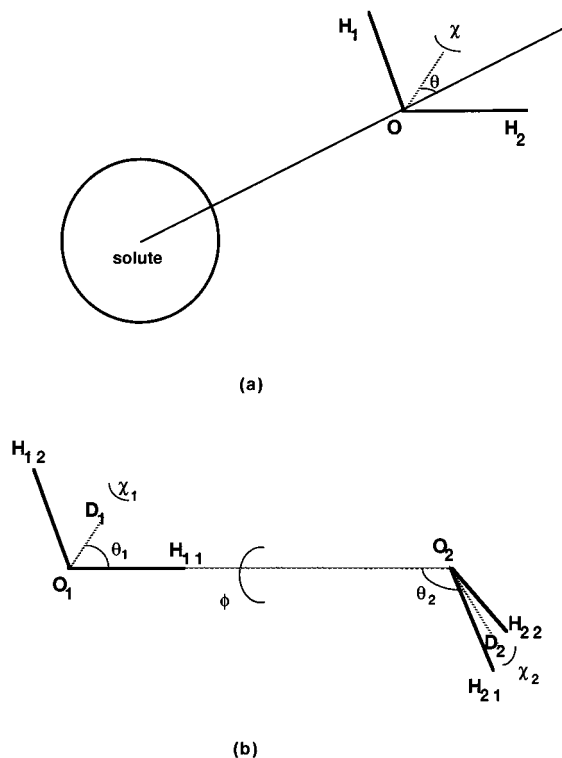


Figure 1. Angles in the (a) solute–water and (b) water–water correlation function.

function (PCF), u_{sw} is the solute–solvent potential, and u_{ww} is the solvent–solvent potential. The values g_{ww}^o and u_{ww} depend on the distance ($R = |\mathbf{r} - \mathbf{r}'|$) and the relative orientation of the two water molecules (ω^{rel} , the five angles defined in Figure 1b, which are a complicated function of $\mathbf{r}, \mathbf{r}', \omega, \omega'$). Here, g_{ww}^{inh} is the inhomogeneous solvent PCF in the mixture, i.e., the correlation function between two solvent molecules given that the solute is at the origin ($\mathbf{r}_s = \mathbf{0}$). It is simply related to the homogeneous triplet correlation function

$$g_{sww}(\mathbf{0}, \mathbf{r}, \mathbf{r}', \omega, \omega') = g_{sw}(\mathbf{r}, \omega) g_{sw}(\mathbf{r}', \omega') g_{ww}^{\text{inh}}(\mathbf{r}, \mathbf{r}', \omega, \omega') \quad (9)$$

The main objective of this work is to estimate the solvent reorganization terms, $\Delta E_{ww}^{\text{cor}}$ and $\Delta S_{ww}^{\text{cor}}$ (eqs 7 and 8), for methane in water. This requires evaluation of integrals over 12 variables specifying the positions and orientations of two water molecules. We do the integration in two stages: we calculate first the integral over the orientations and then the integral over the positions. For this purpose we factor the solute–solvent and solvent–solvent PCF into a radial part and an orientational part,³³ such that

$$g_{sw}(\mathbf{r}, \omega) = g_{sw}^r(\mathbf{r}) g_{sw}^{\text{or}}(\omega | \mathbf{r}) \quad (10)$$

$$g_{ww}(\mathbf{r}, \mathbf{r}', \omega, \omega') = g_{ww}^r(\mathbf{r}, \mathbf{r}') g_{ww}^{\text{or}}(\omega, \omega' | \mathbf{r}, \mathbf{r}') \quad (11)$$

The notation $(\omega | \mathbf{r})$ denotes a conditional distribution function, and, as defined, eqs 10 and 11 are exact. Here g_{sw}^r and g_{ww}^r are the radial distribution functions given by

$$g_{sw}^r(\mathbf{r}) = \frac{1}{\Omega} \int g_{sw}(\mathbf{r}, \omega) d\omega \quad (12)$$

$$g_{ww}^r(\mathbf{r}, \mathbf{r}') = \frac{1}{\Omega^2} \int g_{ww}(\mathbf{r}, \mathbf{r}', \omega, \omega') d\omega d\omega' \quad (13)$$

With this decomposition, the orientationally averaged interaction energy between water molecules in the pure solvent, U^o , can be written as

$$U^o(R) = \frac{1}{\Omega^{\text{rel}}} \int g_{ww}^o(\omega^{\text{rel}} | R) u_{ww}(R, \omega^{\text{rel}}) d\omega^{\text{rel}} \quad (14)$$

where $\Omega^{\text{rel}} = \int d\omega^{\text{rel}}$ and $R = |\mathbf{r} - \mathbf{r}'|$. The orientationally averaged interaction energy for water molecules near the solute, U^m , is

$$U^m(\mathbf{r}, \mathbf{r}') = \frac{1}{\Omega^2} \int g_{sw}^{\text{or}}(\omega | \mathbf{r}) g_{sw}^{\text{or}}(\omega' | \mathbf{r}') g_{ww}^{\text{or,inh}}(\omega, \omega' | \mathbf{r}, \mathbf{r}') \times u_{ww}(R, \omega^{\text{rel}}) d\omega d\omega' \quad (15)$$

With eqs 7, 14, and 15, the solvent reorganization energy is given by

$$\Delta E_{ww}^{\text{cor}} = \frac{1}{2} \rho^2 \int g_{sw}^r(\mathbf{r}) [g_{sw}^r(\mathbf{r}') g_{ww}^{\text{r,inh}}(\mathbf{r}, \mathbf{r}') U^m(\mathbf{r}, \mathbf{r}') - g_{ww}^o(R) U^o(R)] d\mathbf{r} d\mathbf{r}' \quad (16)$$

The integral over \mathbf{r}' of the quantity in brackets in eq 16 is the binding energy relative to the bulk

$$E_b(\mathbf{r}) - E_b^o = \rho \int [g_{sw}^r(\mathbf{r}') g_{ww}^{\text{r,inh}}(\mathbf{r}, \mathbf{r}') U^m(\mathbf{r}, \mathbf{r}') - g_{ww}^o(R) U^o(R)] d\mathbf{r}' \quad (17)$$

where

$$E_b^o = \rho \int g_{ww}^o(R) U^o(R) d\mathbf{r}' = \rho \int g_{ww}^o(R) U^o(R) 4\pi R^2 dR \quad (18)$$

The binding energy is defined as the total interaction of a water molecule with all other water molecules; for pure solvent it is equal to twice the molar energy. With eq 17, eq 16 can be written

$$\Delta E_{ww}^{\text{cor}} = \frac{1}{2} \rho \int g_{sw}^r(\mathbf{r}) [E_b(\mathbf{r}) - E_b^o] d\mathbf{r} \quad (19)$$

This equation was first given by Matubayasi et al.³⁹ Similarly, defining the orientational entropy in pure solvent, S^o , and in the mixture, S^m , as

$$S^o(R) = \frac{1}{\Omega^{\text{rel}}} \int g_{ww}^o(\omega^{\text{rel}} | R) \ln g_{ww}^o(\omega^{\text{rel}} | R) d\omega^{\text{rel}} \quad (20)$$

$$S^m(\mathbf{r}, \mathbf{r}') = \frac{1}{\Omega^2} \int g_{sw}^{\text{or}}(\omega | \mathbf{r}) g_{sw}^{\text{or}}(\omega' | \mathbf{r}') g_{ww}^{\text{or,inh}}(\omega, \omega' | \mathbf{r}, \mathbf{r}') \times \ln g_{ww}^{\text{or,inh}}(\omega, \omega' | \mathbf{r}, \mathbf{r}') d\omega d\omega' \quad (21)$$

the solvent reorganization entropy can be divided into translational and orientational parts, that is

$$\Delta S_{ww}^{\text{cor}} = \Delta S_{ww}^{\text{trans}} + \Delta S_{ww}^{\text{or}} \quad (22)$$

where

$$\Delta S_{ww}^{\text{trans}} = -\frac{1}{2} k \rho^2 \int g_{sw}^r(\mathbf{r}) [g_{sw}^r(\mathbf{r}') \{g_{ww}^{\text{r,inh}} \ln g_{ww}^{\text{r,inh}} - g_{ww}^{\text{r,o}} \ln g_{ww}^{\text{r,o}} - g_{ww}^{\text{r,o}} + 1\} - \{g_{ww}^{\text{r,inh}} \ln g_{ww}^{\text{r,o}} - g_{ww}^{\text{r,o}} + 1\}] d\mathbf{r} d\mathbf{r}' \quad (23)$$

and

$$\Delta S_{\text{ww}}^{\text{or}} = -\frac{1}{2}k\rho^2 \int g_{\text{sw}}^{\text{r}}(\mathbf{r})[g_{\text{sw}}^{\text{r}}(\mathbf{r}')g_{\text{ww}}^{\text{r,inh}}(\mathbf{r},\mathbf{r}') S^{\text{m}}(\mathbf{r},\mathbf{r}') - g_{\text{ww}}^{\text{r,o}}(R)S^{\text{o}}(R)]d\mathbf{r}d\mathbf{r}' \quad (24)$$

where $g_{\text{ww}}^{\text{r,inh}}(\mathbf{r},\mathbf{r}')$ and $g_{\text{ww}}^{\text{r,o}}(R)$ are the radial solvent pair correlation functions in the mixture and in the pure solvent, respectively.

In analogy with the energy, we can define the binding translational and orientational entropies relative to the bulk

$$S_{\text{b}}^{\text{tr}}(\mathbf{r}) - S_{\text{b}}^{\text{tr,o}} = -k\rho \int [g_{\text{sw}}^{\text{r}}(\mathbf{r}')\{g_{\text{ww}}^{\text{r,inh}} \ln g_{\text{ww}}^{\text{r,inh}} - g_{\text{ww}}^{\text{r,inh}} + 1\} - \{g_{\text{ww}}^{\text{r,o}} \ln g_{\text{ww}}^{\text{r,o}} - g_{\text{ww}}^{\text{r,o}} + 1\}]d\mathbf{r}' \quad (25)$$

$$S_{\text{b}}^{\text{or}}(\mathbf{r}) - S_{\text{b}}^{\text{or,o}} = -k\rho \int [g_{\text{sw}}^{\text{r}}(\mathbf{r}')g_{\text{ww}}^{\text{r,inh}}(\mathbf{r},\mathbf{r}') S^{\text{m}}(\mathbf{r},\mathbf{r}') - g_{\text{ww}}^{\text{r,o}}(R)S^{\text{o}}(R)]d\mathbf{r}' \quad (26)$$

The required integrals can be evaluated in two stages: first U^{m} and S^{m} are calculated by integration over orientations at several positions and then the integration over positions is performed.

The radial inhomogeneous solvent–solvent PCF, $g_{\text{ww}}^{\text{r,inh}}(\mathbf{r},\mathbf{r}')$, is related to the homogeneous triplet solute–solvent–solvent correlation function by the radial analogue of eq 9

$$g_{\text{sww}}^{\text{r}}(\mathbf{0},\mathbf{r},\mathbf{r}') = g_{\text{sw}}^{\text{r}}(\mathbf{r}) g_{\text{sw}}^{\text{r}}(\mathbf{r}') g_{\text{ww}}^{\text{r,inh}}(\mathbf{r},\mathbf{r}') \quad (27)$$

This function can be extracted from $g_{\text{sww}}^{\text{r}}$ obtained directly from the simulation. Alternatively, one can employ the Kirkwood Superposition Approximation (KSA), which is equivalent to assuming that the inhomogeneous PCF is equal to the bulk solvent PCF, and depends only on the distance R and the relative orientation ω^{rel} between two solvent molecules

$$g_{\text{ww}}^{\text{r,inh}}(\mathbf{r},\mathbf{r}',\omega,\omega') = g_{\text{ww}}^{\text{o}}(R,\omega^{\text{rel}}) \quad (28)$$

The KSA can be applied separately to the translational and orientational parts of g_{ww} to obtain

$$\text{KSA}^{\text{tr}}: g_{\text{ww}}^{\text{r,inh}}(\mathbf{r},\mathbf{r}') = g_{\text{ww}}^{\text{r,o}}(R) \quad (29)$$

$$\text{KSA}^{\text{or}}: g_{\text{ww}}^{\text{or,inh}}(\omega,\omega'|\mathbf{r},\mathbf{r}') = g_{\text{ww}}^{\text{or,o}}(\omega^{\text{rel}}|R) \quad (30)$$

For nonspherical solutes, calculation of $g_{\text{ww}}^{\text{inh}}$ from the simulation is very difficult and the KSA may be the only option. It is therefore worth examining its performance here where $g_{\text{ww}}^{\text{inh}}$ can be obtained directly.

III. Methods

A. Monte Carlo Simulations. When solvent reorganization properties are to be calculated, the volume of the mixture is critical because the energy and entropy are sensitive functions of the density so that any net compression or expansion of the solvent will affect the calculated solvent–solvent energy and entropy. For example, using the thermodynamic relation

$$\left(\frac{\partial E}{\partial V}\right)_T = T\alpha/\kappa - P \quad (31)$$

and the experimental values for the thermal expansion coefficient ($\alpha = 257.21 \cdot 10^{-6} \text{ K}^{-1}$) and the isothermal compressibility ($\kappa = 45.2472 \cdot 10^{-6} \text{ bar}^{-1}$) of water,⁴⁰ a change in volume of 100 \AA^3 leads to a change in energy of 2.45 kcal/mol , which is of the order of the ΔE_{ww} to be calculated. Constant pressure simulations are preferable but cost more CPU time (about 15%

more) and probably converge more slowly due to sampling of the volume as an additional variable.

The simulations at 25°C were performed at constant volume. For the pure solvent the simulations included 216 molecules, at density $\rho = 0.03302 \text{ \AA}^{-3}$, and averages over 20 million configurations were calculated. For the mixture, care was required to avoid a significant change in the density. Consequently, a methane particle was added and two water molecules were removed because the partial molar volume of methane in water at room temperature ($62 \text{ \AA}^3/\text{molecule}$ ⁴¹) is approximately equal to twice the molar volume of water (30 \AA^3). Averages were calculated for 80 million configurations. Since the partial molar volume of methane is not known at the higher temperatures, the simulations at 65 and 160°C were performed at a constant pressure of 1 and 6.1 atm , respectively (216 molecules, 10 million configurations for pure water; 214 water molecules + 1 methane particle, 60 million configurations for the mixture). Here, 6.1 atm corresponds to the experimental saturated liquid at 160°C . All equilibrations lasted at least 1 million configurations for the pure fluids and 10 million configurations for the mixtures. The average density at 65 and 160°C was 0.03232 and 0.02862 \AA^{-3} , respectively.

All simulations were carried out with the program BOSS⁴² modified to calculate additional structural properties (see below). The TIP4P model was used for water⁴³ because it is more accurate than TIP3P or SPC, particularly at higher temperatures (Mackerell and Karplus, unpublished). Methane was represented by a Lennard-Jones (LJ) particle ($\sigma = 3.73 \text{ \AA}$, $\epsilon = 0.294 \text{ kcal/mol}$ ⁴⁴) with geometric average combining rules for the solute–solvent interaction. Periodic boundary conditions and preferential sampling were employed with the interactions truncated at 8.5 \AA by smooth quadratic switching from 8 \AA . These choices for the simulation parameters are in accord with the implementation of Jorgensen in the BOSS program.

For the mixture simulations, the following quantities were calculated:

- (a) Solute–water oxygen radial distribution function g_{sw}^{r} .
- (b) Water orientational distribution with respect to the solute $g_{\text{sw}}^{\text{or}}$. This calculation was done as before¹⁵ in four regions: three subshells of the first solvation shell (first, $r < 3.8 \text{ \AA}$; second, $3.8 < r < 4.6 \text{ \AA}$; and third, $4.6 < r < 5.4 \text{ \AA}$) and the second solvation shell ($5.4 < r < 7.4 \text{ \AA}$). The definition of the angles $\omega = (\theta, \chi)$ is given in ref 14 (see Figure 1a).
- (c) Triplet solute–water oxygen–water oxygen correlation function. This is a function of three distances: r is the distance of the first water molecule (the oxygen taken as center) from the solute, s the distance of the second water molecule from the solute and t the distance between the two water molecules. A histogram $x(r,s,t)$ of r,s,t values at 0.1 \AA intervals was calculated from the simulations at each temperature for $r,s,t \leq 7.4 \text{ \AA}$. The triplet correlation function was obtained from the expression

$$g_{\text{sww}}(r,s,t) = \frac{x(r,s,t)}{N_{\text{conf}} \Delta V(r,s,t) \rho^2} \quad (32)$$

where N_{conf} is the number of configurations, ΔV is the volume element corresponding to the r,s,t values, calculated according to the formulas given by Krumhansl and Wang,⁴⁵ and ρ the pure solvent number density.

(d) Solvent–solvent orientational correlation functions for nearest neighbor water molecules in three regions: S1S1W1, S1S2W1, and S2S2W1, where S1 and S2 denote the first and second solvation shell of the solute, respectively, and W1

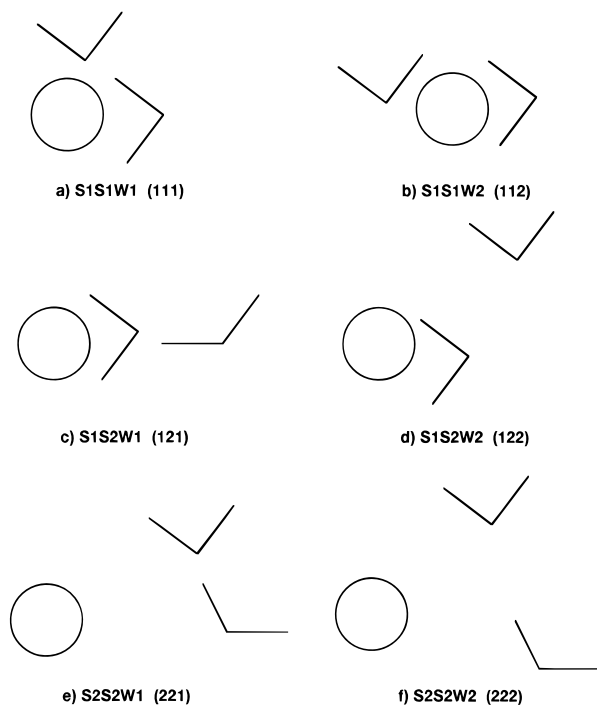


Figure 2. Configurations of a solute-water-water triplet.

denotes the first water-water neighbor shell ($t < 3.4$ Å) (see Figure 2). S1S1W1, for example, means that the two solvent molecules are in the first shell with respect to the solute and also in the first shell with respect to each other (Figure 2a). The correlation functions calculated are one- and two-dimensional marginal distributions of the five relative water-water angles, $\omega^{\text{rel}} = (\theta_1, \theta_2, \phi, \chi_1, \chi_2)$. These angles are defined as follows (see Figure 1b):³³ θ_1 and θ_2 are the angles between the water dipole vectors and the axis connecting the oxygen atoms of each molecule; ϕ describes rotation of the dipole vectors around this axis; χ_1 and χ_2 describe rotation of each water molecule around its dipole vector. Histograms of these functions at 10° intervals were accumulated during the simulations. The same marginal distribution functions for pure solvent at a number of temperatures have been calculated before.³³

(e) Binding energy of water molecules (interaction with all other water molecules) as a function of distance from the solute.

(f) Average water-water pair interactions in six regions: S1S1W1, S1S1W2, S1S2W1, S1S2W2, S2S2W1, S2S2W2, where W2 denotes the second water-water solvation shell ($3.4 < t < 5.6$ Å); see Figure 2.

B. Approximations for g_{ww} . Whereas the solvent reorganization energy and other energetic quantities can be obtained directly from a simulation, the calculation of the entropy requires knowledge of the correlation functions (see eqs 6 and 8). The solvent reorganization entropy requires the pure and inhomogeneous water-water PCF, as shown in eq 8. The bulk water-water PCF is a function of six variables, the distance R and the five angles ω^{rel} , and cannot be obtained directly from a simulation due to the large amount of data required for convergence. Two approximations were developed recently and have been used for the analysis of the entropy of pure water.³³

Factorization in Terms of Lower Dimensionality Marginal Distributions (FAC Approximation). In ref 33, a number of factorizations of $g_{\text{ww}}^{\text{or}}$ were tested. The following factorization was found to be most satisfactory for calculation of the pure water entropy

$$g_{\text{ww}}^{\text{or}}(\theta_1, \theta_2, \phi, \chi_1, \chi_2) \approx g(\theta_1, \theta_2) g(\chi_1, \chi_2) g(\theta_1, \chi_2) g(\chi_1, \theta_2) \times g(\phi) / g(\theta_1) g(\chi_1) g(\theta_2) g(\chi_2) \quad (33)$$

although it underestimates the magnitude of the energy. For pure water at a number of temperatures, the correlation functions that appear in eq 33 were calculated in three regimes of R : first subshell ($R < 2.8$ Å) and second subshell ($2.8 < R < 3.4$ Å) of the first solvation shell, and the second shell ($3.4 < R < 5.6$ Å).³³ To obtain a smooth function of R , an interpolation scheme was introduced. The calculated distributions in the above three regions are “assigned” to $r_1 = 2.7$, $r_2 = 3.1$, $r_3 = 4.6$ Å, respectively; they are referred to as g_1 , g_2 , and g_3 , respectively. For $R \leq r_1$, we use the first subshell distribution; for $r_1 < R < r_2$ we do a linear interpolation between the values for r_1 and r_2 ; for $r_2 < R < r_3$ we do a nonlinear interpolation to match the behavior of the orientationally averaged pair interaction energy obtained directly from the simulation (Figure 3). It was found that the function

$$g = g_2 + (g_3 - g_2) b \left(\frac{r - r_2}{r_3 - r_2} \right)^{1/10} \quad (34)$$

yielded satisfactory results. For $R > r_3$ we smoothly decrease g to unity:

$$g = 1 + (g_3 - 1) \left(\frac{r_3}{r} \right)^6 \quad (35)$$

The molar energy of pure water at 25 °C and 1 atm calculated with this approximate PCF is -7.85 kcal/mol, compared to -10.1 kcal/mol obtained directly from the simulation. The discrepancy is due to the slight underestimation of the magnitude of U^0 over most of the range of distances and is a limitation of the factorization approximation to g_{ww} for the energy.

AGP (Adjusted Gas Phase) Approximation. This approximation uses the gas phase g_{ww} (eq 36) as a reference and adjusts it to reproduce the liquid phase orientationally averaged interaction (eq 37) and certain marginal distributions obtained from the simulation (eq 39)

$$g^{\text{gas}}(\omega^{\text{rel}}|R) = \frac{\exp(-u_{\text{ww}}/kT) \Omega^{\text{rel}}}{\int \exp(-u_{\text{ww}}/kT) d\omega^{\text{rel}}} \quad (36)$$

$$g^{\text{s}}(\omega^{\text{rel}}|R) = g^{\text{gas}}(\omega^{\text{rel}}|R) + s(R) (1 - g^{\text{gas}}(\omega^{\text{rel}}|R)) \quad (37)$$

where

$$s(R) = \frac{U^0[R; \text{simul}] - U^0[R; g^{\text{gas}}]}{\langle U \rangle_{\text{R}} - U^0[R; g^{\text{gas}}]} \quad (38)$$

and $\langle U \rangle_{\text{R}}$ is an unweighted average over orientations ($\langle U \rangle_{\text{R}} = 1/\Omega^{\text{rel}} \int u_{\text{ww}}(R, \omega^{\text{rel}}) d\omega^{\text{rel}}$).

With these assumptions we have

$$g^{\text{AGP}}(\theta_1, \theta_2, \phi, \chi_1, \chi_2|R) = g^{\text{s}}(\theta_1, \theta_2, \phi, \chi_1, \chi_2|R) \times \delta g(\theta_1, \theta_2|R) \times \delta g(\chi_1, \chi_2|R) \times \delta g(\phi|R) \quad (39)$$

where, for example,

$$\delta g(\theta_1, \theta_2|R) = g^{\text{liq}}(\theta_1, \theta_2|R) / g^{\text{s}}(\theta_1, \theta_2|R) \quad (40)$$

and g^{liq} is obtained from the simulation. The functions δg are calculated in three regions: first and second subshell of first neighbor shell, and in the second shell (see above). The molar

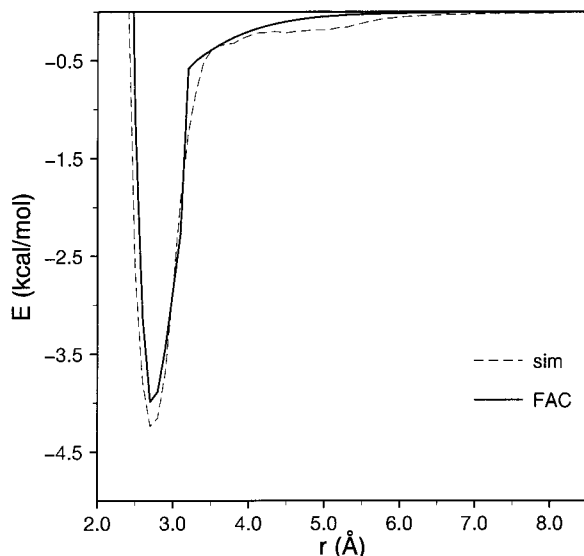


Figure 3. Orientationally averaged interaction energy from simulation (dashed line) and from the factorization approximation to g_{ww} .

energy calculated with g^{AGP} is -10.1 kcal/mol, in good agreement with the simulation. This good agreement is partly due to a compensation of underestimating U^o at short distances and overestimating it at longer distances (see Figure 3 of ref 33).

The above two approximations for $g_{\text{ww}}^{\text{or}}$ were developed primarily for the entropy and are not very accurate for energy calculations (especially FAC, as pointed out above). Therefore, they should not be expected to perform very accurately in solvent reorganization energy calculations, although some cancellation of errors occurs because the difference between the solvent energy in the mixture and in the pure solvent is taken.

C. Integration over Orientations. Equations 15 and 21 for the calculation of U^{m} and S^{m} require integrations over six angular variables. Whereas a product rule was used for integration over five degrees of freedom in Lazaridis and Karplus,³³ a nonproduct rule is used here for increased efficiency. A number of multidimensional integration methods were tested: standard Monte Carlo,⁴⁶ adaptive Monte Carlo,⁴⁷ Conroy's number theoretical method,⁴⁸ and the embedded lattice rule of Sloan and Joe,⁴⁹ which is an extension of Conroy's method. The method of Sloan and Joe was chosen as the best combination of accuracy and efficiency. During testing, 320 192 sample points were used for the evaluation of each integral. The independent variables in the integrals were the water orientations with respect to the solute (ω, ω'). From these and the positions of the water molecules, the relative water–water angles (ω^{rel}) were calculated.

As in the case of $g_{\text{ww}}^{\text{or}}$ (see above), an interpolation scheme for $g_{\text{sw}}^{\text{or}}$ is used in these integrations. The four calculated distributions are assigned to $r_1 = 3.6$, $r_2 = 4.2$, $r_3 = 5.0$, and $r_4 = 6.5$ Å, and linear interpolation is done for distances between r_1 and r_4 . For $r < r_1$ the first subshell distribution is used and for $r > r_4$ smooth extrapolation to unity is performed

$$g = 1 + (g_4 - 1) \left(\frac{r_4}{r} \right)^6 \quad (41)$$

The functions $g_{\text{sw}}^{\text{or}}(\omega|\mathbf{r})$, $g_{\text{sw}}^{\text{or}}(\omega'|\mathbf{r}')$, $g_{\text{ww}}^{\text{or,inh}}(\omega, \omega'|\mathbf{r}, \mathbf{r}')$ and $g_{\text{ww}}^{\text{or,inh}}(\omega, \omega'|\mathbf{r}, \mathbf{r}')$ are normalized so that their integral over orientations is equal to Ω^2 .

D. Integration over Positions. Since we are considering a monatomic, spherically symmetric solute, the integrals over \mathbf{r} and \mathbf{r}' can be reduced from six to three dimensions by using spherical coordinates for $d\mathbf{r} \rightarrow 4\pi r^2 dr$ and bipolar coordinates for $d\mathbf{r}' \rightarrow 2\pi/r s ds t dt$ so that $d\mathbf{r}d\mathbf{r}' = 8\pi^2 r dr s ds t dt$. The integration over r, s, t is performed using the extended trapezoidal rule.⁴⁶ The integration domain can be divided up such that the contribution from certain ranges of r, s, t values can be calculated. These regions are characterized by three integers: ir, is, it . Here $ir = 1$ corresponds to $r < 5.4$ Å (first shell), $ir = 2$ to $5.4 < r < 7.4$ Å (second shell), and $ir = 3$ to $r > 7.4$ Å; $is = 0$ corresponds to the excluded volume region ($s < 2.7$ Å), $is = 1$ to $2.7 < s < 5.4$ Å, $is = 2$ to $5.4 < s < 7.4$ Å, and $is = 3$ to $s > 7.4$ Å; $it = 1, 2, 3$ corresponds to the first water–water shell ($t < 3.4$), the second water–water shell ($3.4 < t < 5.6$ Å) and beyond the second shell, respectively. For example, the region ($ir = 1, is = 1, it = 1$) = (111) corresponds to S1S1W1 in Figure 2.

Since $U^{\text{m}}(r, s, t)$ and $S^{\text{m}}(r, s, t)$ can be calculated only at a limited number of points, an interpolation scheme is needed for all other r, s, t values. Calculation of $U^{\text{m}}, S^{\text{m}}$ was done at eight values of r and s (from 2.941 to 7.692 Å) and 15 values of t (from 2.439 to 7.692) for triplets satisfying the triangle inequality. The (r, s, t) points were spaced evenly on a $(1/r, 1/s, 1/t)$ grid so that more evaluations were done at smaller solute–solvent and solvent–solvent distances where most of the contributions to the integrals arise.⁵⁰ For example, $1/r$ is sampled from 0.13 to 0.34 at constant intervals of 0.03, corresponding to the r values 7.692, 6.25, 5.263, 4.545, 4, 3.571, 3.226, 2.439. Also, for every r, t pair, evaluation was done at $s = r - t$, and for every s, t pair, at $r = s + t$ to improve the interpolation. There was a total of 543 integral evaluations (due to symmetry only $s \leq r$ points need to be calculated). For interpolations in regions close to a linear arrangement of (r, s, t) points that violated the triangle inequality were replaced by the closest linear arrangement.

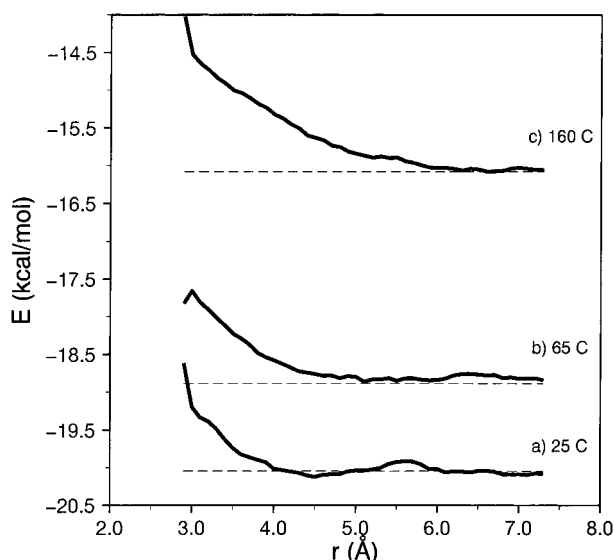
IV. Results

A. Energetics Obtained Directly from Simulation. The most straightforward method for calculating the solvent reorganization energy is to take the difference between the solvent–solvent energy in the mixture and the energy of an equal number of solvent molecules from a pure solvent simulation (see, for example, refs 7, 12, 20, 19). This difference is the total solvent reorganization energy, i.e., it includes the small liberation contribution. This approach has a major limitation in its large statistical uncertainty due to taking the difference of two large, fluctuating numbers. The values calculated in this way are shown in Table 1 for simulations at 25, 65, and 160 °C. The solvent reorganization energy is slightly negative at 25 °C and positive at 65 and 160 °C, but the error bars are substantial.

An alternative and more informative method for calculating $\Delta E_{\text{ww}}^{\text{cor}}$ is by integration of the water binding energy, $E_b(r)$, relative to the bulk, E_b^o (eq 19). This method is more precise because it focuses on the region around the solute, and the difference is not influenced by the energy fluctuations of the solvent far away. At 25 °C, $E_b(r)$ for small r (close to methane) is much less negative than bulk, E_b^o ; it becomes slightly more negative than bulk at about 4.5 Å, exhibits a maximum around the first minimum of the RDF (around 5.4 Å), and reaches the bulk value in the second solvation shell (Figure 4a). The average binding energy of the waters in the first solvation shell ($r \leq 5.4$ Å) is -19.96 ± 0.2 kcal/mol and in the second solvation shell ($5.4 \leq r \leq 7.4$ Å) is -20.05 ± 0.1 kcal/mol. The bulk value from pure solvent simulations is -20.05 ± 0.04 kcal/

TABLE 1: Energetics Directly from the Simulation (kcal/mol)^a

	25 °C	65 °C	160 °C
Solvent Reorganization Energy			
total energy	-2150.6 ± 6.5	-2018.7 ± 5.6	-1716.9 ± 6.3
E_{sw}	-2.945 ± 0.1	-2.679 ± 0.15	-2.18 ± 0.1
$E_{ww} = E - E_{sw}$	-2147.65 ± 6.5	-2016.0 ± 5.6	-1714.7 ± 6.3
E_{ww}^o	-2144.9 ± 4.1	-2020.85 ± 1	-1720.4 ± 11.6
$\Delta E_{ww} = E_{ww} - E_{ww}^o$	-2.8 ± 7.7	4.82 ± 5.7	5.67 ± 13.2
ΔE_{ww} (from eq 19)	0.87 ± 2.7	4.08 ± 2.4	6.46 ± 4.5
Average Water–Water Binding Energies			
$\langle B \rangle$ first shell	-19.96 ± 0.2	-18.61 ± 0.13	-15.48 ± 0.26
$\langle B \rangle$ second shell	-20.05 ± 0.1	-18.81 ± 0.1	-16.03 ± 0.13
$\langle B \rangle$ bulk	-20.05 ± 0.04	-18.886 ± 0.01	-16.08 ± 0.11
Average Water–Pair Interaction Energies			
S1S1W1	-3.63 ± 0.2	-3.36 ± 0.06	-3.05 ± 0.04
S1S2W1	-3.17 ± 0.09	-2.95 ± 0.03	-2.74 ± 0.05
S2S2W1	-3.23 ± 0.2	-2.996 ± 0.06	-2.80 ± 0.05
S1S1W2	-0.24 ± 0.03	-0.23 ± 0.017	-0.26 ± 0.01
S1S2W2	-0.23 ± 0.01	-0.23 ± 0.011	-0.24 ± 0.01
S2S2W2	-0.24 ± 0.04	-0.215 ± 0.013	-0.24 ± 0.01
bulk W1	-3.09 ± 0.03	-2.98 ± 0.04	-2.76 ± 0.001
bulk W2	-0.21 ± 0.004	-0.20 ± 0.01	-0.22 ± 0.001

^a Statistical uncertainties calculated by block averages.**Figure 4.** Water binding energy as a function of distance from the solute at (a) 25 °C (b) 65 °C, and (c) 160 °C.

mol. Thus, even in the first shell, the water binding energy is close to that in the bulk.

This result for $E_b(r)$ is qualitatively similar to that obtained for methane in ST2 water,³⁹ but there are quantitative differences. The minimum of $E_b(r)$ in the first shell is deeper in that work (~ 0.4 kcal/mol less than E_b^o) and the maximum is higher (~ 0.21 kcal/mol higher than E_b^o). Also, there is a minimum at about 8 Å from the solute (~ 0.14 less than E_b^o). This is beyond the range examined here, but the binding energy seems to have converged to the bulk value by 7.4 Å within the accuracy of the calculations. Part of the difference is attributable to the difference in temperature (10 °C used by Matubayasi et al. vs 25 °C here), but most of it is probably due to the different water models.⁵¹ ST2 water has long been known to be too “tetrahedral”.⁵² Also, because the density maximum of ST2 is at 27 °C,⁵³ simulation of ST2 at a given temperature is in some ways equivalent to simulating water at much lower temperature.⁵⁴ Other simulations with ST2 have shown that the binding energy in the first shell is significantly more negative by 0.64 to 0.67 kcal/mol than in the bulk,^{10,18} in contrast to the TIP4P results

presented here. A deep minimum was also not found for krypton in TIP3P water at 300 K.¹⁹ At 65 °C the oscillations in $E_b(r)$ are diminished relative to room temperature (Figure 4b). The average binding energy in the first shell is -18.61 ± 0.13 and in the second shell -18.81 ± 0.1 kcal/mol. The bulk value is -18.886 ± 0.01 . At 160 °C the binding energy relative to the bulk is higher in the first solvation shell and monotonically decreases to zero in the second solvation shell (Figure 4c).

The values of ΔE_{ww}^{cor} obtained from the integration of the binding energy are given in Table 1. Since the difference in binding energy between the first shell and bulk increases with temperature, there is an increase in ΔE_{ww}^{cor} with temperature. Integration of eq 19 up to 7.3 Å gives 0.87 kcal/mol at 25 °C, 4.08 kcal/mol at 65 °C, and 6.46 kcal/mol at 160 °C. The statistical uncertainty of these values is considerable but smaller than that of the difference in water–water energy between the mixture and pure solvent simulations. For comparison, a value of about 2 kcal/mol was found for ΔE_{ww} at 25 °C by Durell and Wallqvist¹⁹ (their calculation gives ΔE_{ww} , not ΔE_{ww}^{cor}).

The heat capacity of hydration, when written as the temperature derivative of the solvation enthalpy, can be decomposed as

$$\Delta C_p = \left(\frac{\partial \Delta H}{\partial T} \right)_p = \frac{\partial E_{sw}}{\partial T} + \frac{\partial \Delta E_{ww}}{\partial T} + P \frac{\partial \Delta V}{\partial T} \quad (42)$$

where the last term is negligible under ambient conditions. If we estimate the remaining two derivatives in eq 42 as finite differences between 25 °C and 160 °C using for ΔE_{ww} ($\Delta E_{ww} \approx \Delta E_{ww}^{cor}$), the values obtained from integration of the binding energy profile (eq 19), we obtain for the excess heat capacity contributions

$$\Delta C_{p,sw} = 5.64 \pm 1 \text{ cal/mol K}$$

$$\Delta C_{p,ww} = 41.3 \pm 40 \text{ cal/mol K}$$

The experimental value for ΔC_p is about 50 cal/mol K.^{55,56} Although the values have large statistical uncertainties (e.g., if we use the 25 °C and 65 °C results, $\Delta C_{p,ww} = 80$ cal/mol K), the major contribution to ΔC_p clearly comes from the increase in ΔE_{ww} with temperature. This is in agreement with other simulation studies.^{57,58}

Average water–water pair energies are also listed in Table 1 (see section IIIA and Figure 2 for definition of S1S1W1 etc.). At 25 °C, first neighbor water–water interactions are more negative than in the bulk for all three regions studied, particularly in region S1S1. This “enhancement” of pair interactions in S1S1 has been found in many previous simulations.^{7,10,18,19} The strong enhancement in region S1S1 is due to the fact that a pair of water molecules placed next to a “noninteracting” particle is “allowed” to hydrogen bond more than if they were in the bulk where they could interact with neighboring water molecules. An even greater enhancement of the mutual interaction results if the two molecules are placed in vacuum (as long as they maintain the same partial charge distribution as in the liquid) (see Figure 3 of ref 33). The fact that pair energies are more negative than in the bulk is not inconsistent with the fact that the binding energy of water molecules in the first shell is less negative than for water molecules in the bulk; the binding energy in the first shell refers to the interactions of a water molecule in the first shell of methane with all other water molecules. These water molecules have fewer neighbors around them due to the volume excluded by the solute.¹⁸ As the temperature increases, the difference

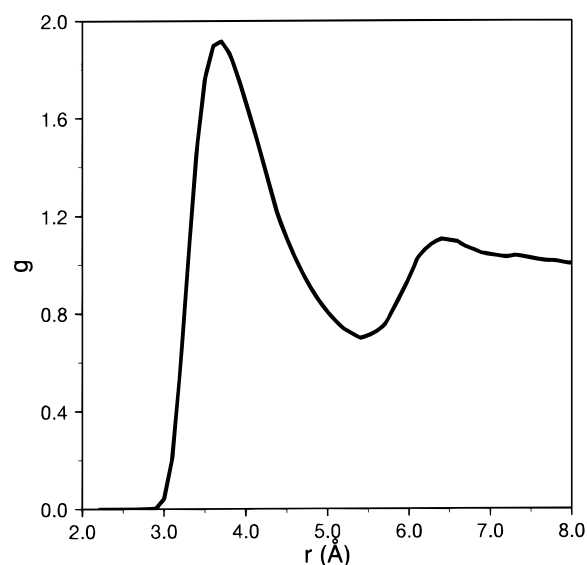


Figure 5. Methane–water oxygen radial distribution function at 25 °C.

between the pair energies in S1S1W1 and in the bulk diminishes. This is due to flattening of $g_{\text{sw}}^{\text{or}}$ with increasing temperature. In the limit of $g_{\text{sw}}^{\text{or}} = 1$, the two would become identical within the KSA^{or} (see eqs 14, 15).

An energetic analysis of methane solvation as a function of temperature has been reported by Bridgeman et al.⁵⁷ Although the potential energy function used there is the same as in the present study, some differences are apparent. First, they find a decrease in water–water structure across the first shell–second shell interface. This is not found here: S1S2 pair interactions are slightly more negative than bulk at 25 °C and essentially the same as bulk at 65 °C and 160 °C. Also, the water–water correlation functions are very similar to bulk (see next section). Second, the difference between average pair interaction between S1S1 and bulk remains constant in the Bridgeman et al. simulations up to 120 °C, whereas it decreases in the present study. Finally, the difference in binding energy between the first solvation shell and the bulk starts decreasing above 57 °C in their simulations, which is not consistent with the fact that the experimental hydration heat capacity is still positive at such temperatures. For the three temperatures studied here, the difference in binding energy between first solvation shell and bulk increases with temperature. The origin of the differences between the two sets of simulations is not clear. However, it should be noted that the results of Bridgeman et al. are based on direct averaging of interaction energies rather than correlation function analysis. In our work, the former leads to much larger uncertainties than the latter (see above).

B. Correlation Functions. 1. Solute–Solvent Correlation Function. The methane–water radial distribution function is readily calculated from the simulations and has been repeatedly reported (see, for example, ref 14). This RDF at 25 °C is shown in Figure 5. It becomes less structured with increasing temperature.^{14,28} The orientational correlation functions for the three subshells of the first solvation shell and the second shell have also been reported.¹⁵ Figure 6 shows this correlation function for the first subshell at 25 °C. As observed in many simulations^{7–17} and recently confirmed experimentally,⁵⁹ the preferred orientations in the first solvation shell are those with a hydrogen or a lone pair pointing away from the solute (“straddling” orientation). In the second shell a weak preference toward the opposite orientation is observed. All distributions

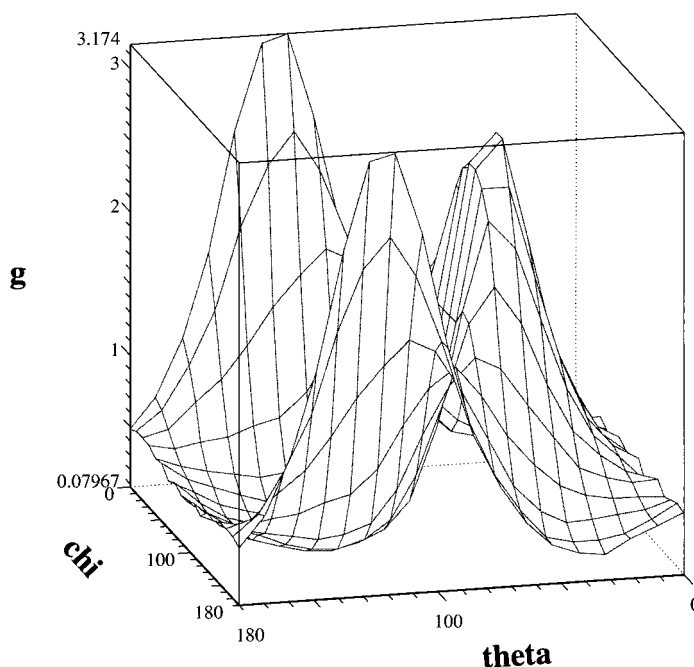


Figure 6. Methane–water orientational correlation function at 25 °C in the first subshell of the first solvation shell ($r < 3.8$ Å).

become flatter as the temperature increases. However, even at 160 °C a preference for the “straddling” water orientation in the first solvation shell persists, although it is significantly weaker than at room temperature. For example, in the first subshell, the maximum of $g_{\text{sw}}^{\text{or}}(\theta, \chi)$ at 25 °C occurs at $\theta = 115^\circ$, $\chi = 0^\circ$ and is equal to 3.17; the maximum at 160 °C occurs at $\theta = 125^\circ$, $\chi = 0^\circ$ and is equal to 1.85. This weakening of orientational correlations is also reflected in the behavior of the site–site correlation functions as the temperature is increased.²⁸

2. Solute–Water–Water Radial Triplet Correlation Function. The deviation of the radial triplet correlation function $g_{\text{sww}}^{\text{r}}$ between methane and the oxygen atoms of two water molecules from the KSA^r (eqs 27 and 29) was obtained from the solute–solvent and the solvent–solvent radial distribution functions

$$\delta g_3(r, s, t) = \frac{g_{\text{sww}}^{\text{r}}(r, s, t)}{g_{\text{sw}}^{\text{r}}(r)g_{\text{sw}}^{\text{r}}(s)g_{\text{ww}}^{\text{r}, \text{o}}(t)} \quad (= 1 \text{ for KSA}^{\text{r}}) \quad (43)$$

From eqs 43 and 27, we obtain

$$g_{\text{ww}}^{\text{r}, \text{inh}} = g_{\text{ww}}^{\text{r}, \text{o}} \delta g_3(r, s, t) \quad (44)$$

The deviation is a more sensitive function than $g_{\text{sww}}^{\text{r}}$ itself. Four slices of δg_3 at 25 °C are plotted in Figure 7. They are $\delta g_3(3.7, 3.7, t)$, $\delta g_3(3.7, s, 2.8)$, $\delta g_3(6.4, 6.4, t)$, $\delta g_3(6.4, s, 2.8)$ where 3.7 and 6.4 Å correspond to the first and second peaks of the solute–water RDF and 2.8 Å is the first peak of the water–water RDF.^{43,33}

Figure 7a shows the relative probability, with respect to KSA^r, of observing a distance t between two water molecules which are both 3.7 Å from the solute. Significant enhancement of the probability of the first neighbor peak is observed ($\delta g_3 = 1.415$ at $t = 2.8$ Å). There is also enhanced probability at $t = 5$ Å (corresponding to molecules separated by another water molecule). The population in the region of the minimum in the bulk water radial distribution function is further reduced next to methane ($\delta g_3 = 0.64$ at $t = 3.6$). Figure 7b shows the relative

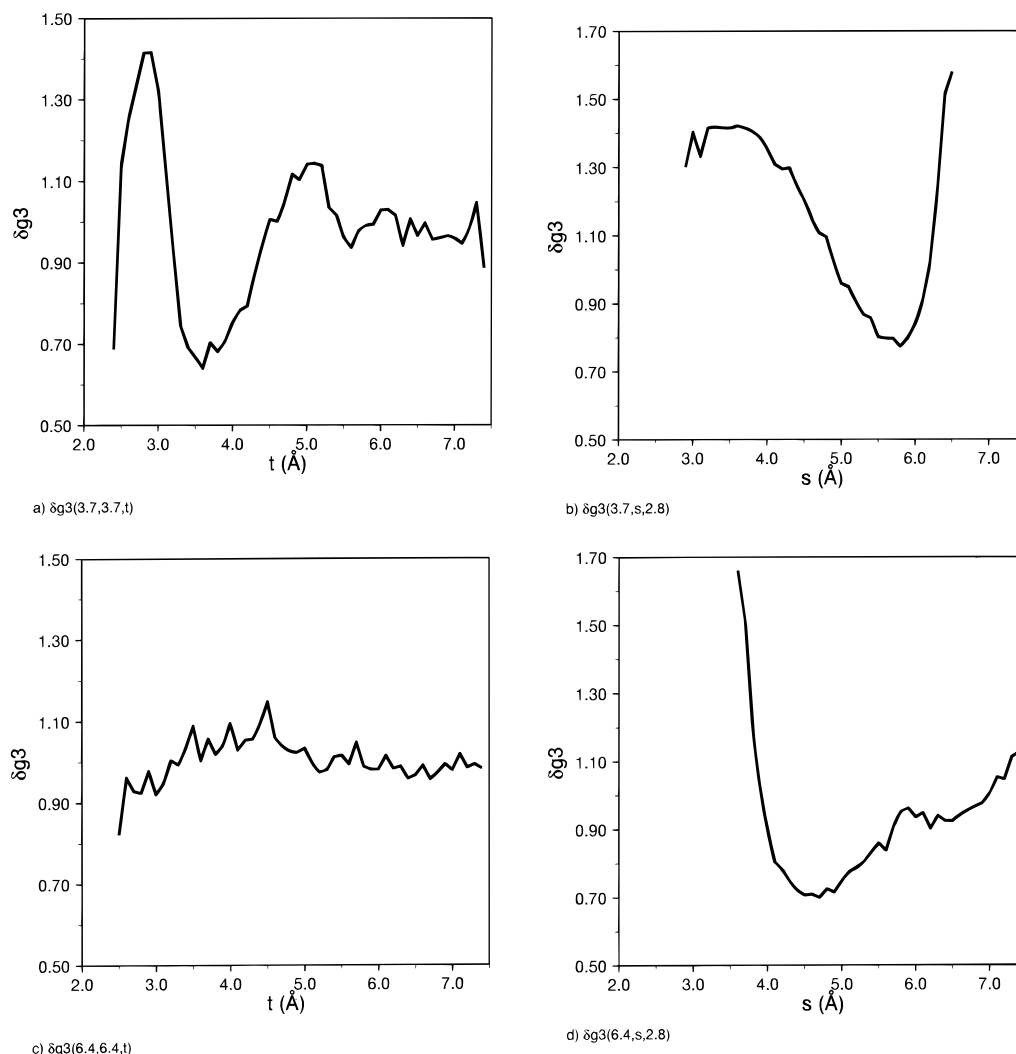


Figure 7. Four slices of the radial triplet solute–water–water correlation function at 25 °C: (a) $\delta g_3(3.7,3.7,t)$; (b) $\delta g_3(3.7,s,2.8)$; (c) $\delta g_3(6.4,6.4,t)$; (d) $\delta g_3(6.4,s,2.8)$.

probability of s given $r = 3.7$ Å and $t = 2.8$ Å. The two peaks in this function correspond to the two hydrogen bonding partners of a first-shell water molecule, one in the first shell ($s \sim 3.7$ Å) and the other in the second shell ($s \sim 6.5$ Å). Figure 7c shows the relative probability of t for $r = s = 6.4$ Å. There is little structure in this slice of δg_3 , although there is a slight reduction in probability of the first water–water peak and enhancement at intermediate distances (3.5 to 5 Å). Finally, Figure 7d shows the probability of s for $r = 6.4$ and $t = 2.8$ Å. There is significant structure with enhancement of probability at the first shell position, $s = 3.7$ Å and next the position $s = 7.4$ Å. The second shell molecules have a slight preference for orientations where a hydrogen or a lone pair points toward the solute.¹⁵ This would predispose them for hydrogen bonding with third solvation shell water molecules at an angle of 109° from the solute–water direction, which, for $t = 2.8$ Å, would place them at a distance from the solute of about 7.8 Å. Overall, the deviations from KSA^{tr} can be explained in terms of the preferred orientations of first solvation shell water molecules with respect to the solute. The positions around a first shell water molecule that correspond to tetrahedral coordination (hydrogen bonding) have enhanced probability compared to other directions. This suggests that a simple model for δg_3 based on the known g_{sw}^{or} could be constructed, though we do not do so here. The consequences

on the entropy of the deviations from the KSA^{tr} described here are discussed in section IVC2.

At 65 °C and 160 °C, δg_3 is qualitatively similar but less structured (not shown). For example, the peak at 3.7,3.7,2.9 decreases from 1.416 at 25 °C to 1.328 at 65 °C and 1.193 at 160 °C and the minimum at 3.7,3.7,3.6 increases from 0.64 at 25 °C to 0.819 at 65 °C and 0.893 at 160 °C. The reduction in structure of δg_3 is linked to the reduction in structure of g_{sw}^{or} (section B1).

3. Water–Water Orientational Correlations. First neighbor ($t \leq 3.4$ Å, where t is the distance between water molecules) water–water orientational distribution functions were calculated in three regions: S1S1, S1S2, S2S2 (see Figures 1 and 2). The results for the one-dimensional marginal correlation functions $g(\theta)$, $g(\chi)$, and $g(\phi)$ for 25 °C are shown in Figures 8–10 and compared to the corresponding functions for pure solvent.³³ The two-dimensional functions (not shown) are very similar to those for bulk water; for the latter see.³³ In S1S1 (Figure 8) there is a significant increase in the hydrogen bonding orientations of $g(\theta)$ ($\theta = 50^\circ$ or 150°); the χ distribution also exhibits an increase in the probability of hydrogen bonding donor configurations ($\chi = 90^\circ$) while the ϕ distribution is essentially flat for both pure solvent and the mixture. At 65 °C the distributions are similar (not shown) but less structured for both the pure

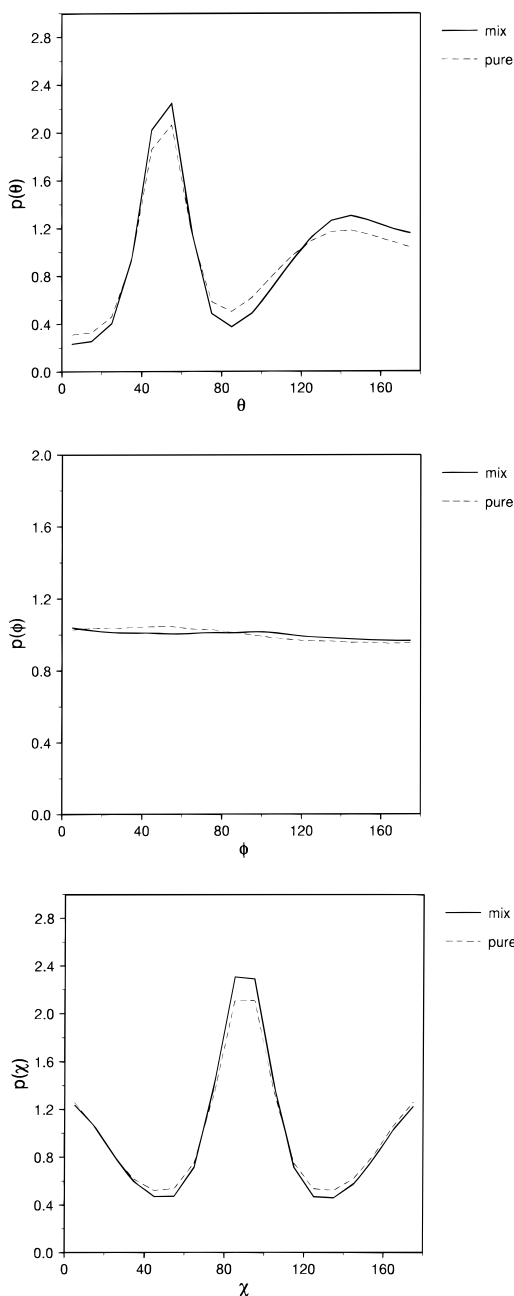


Figure 8. Water–water orientational correlations in region S1S1W1 (both in first solvation shell) at 25 °C: (a) $g(\theta)$; (b) $g(\phi)$; (c) $g(\chi)$.

fluid and the mixture, and the difference between the two is somewhat smaller. The ϕ distribution shows a slight preference for parallel dipole configurations ($\phi = 0$) for both pure solvent and the mixture.

In Figure 9 we plot separately $g(\theta)$ and $g(\chi)$ for the two S1S2 water molecules in Figure 2 because they are not equivalent. Subscript 1 refers to the molecule in the first shell and subscript 2 to the molecule in the second shell. All of the distribution functions are very close to the pure solvent functions. There is slight enhancement of $g(\chi_1)$ at $\chi_1 = 90^\circ$ and 0° and $g(\theta_1)$ near $\theta_1 = 50^\circ$ and a marked decrease in the high values of θ_1 ($\theta_1 > 140^\circ$). The distributions of θ_2 and χ_2 are essentially identical to the bulk distributions. In ϕ there is a slight enhancement of parallel-dipole configurations in the mixture. The results at 65 °C are similar, except that the slight enhancement in $g(\chi_1)$ at 90° and $g(\theta_1)$ at 50° is not observed and $g(\chi_2)$ at 90° is actually

less structured than in the bulk. In Figure 10, which shows the results for S2S2, there is a slight enhancement in the hydrogen bonding configurations at 25 °C, but at 65 °C (not shown) the distribution functions are essentially identical to those of pure water. In all regions, the results at 160 °C (not shown) are similar to those at 65 °C, although both the pure and mixture distribution functions are less structured.

Triplet Correlation Functions. The angles ω and ω' in eq 8 describe the orientation of two water molecules with respect to the solute. The solute–solvent orientational distribution, g_{sw}^{or} , is naturally given in terms of these angles. The orientational triplet solute–water–water correlation function (at fixed positions of the two water molecules, $\mathbf{r}_1, \mathbf{r}_2$) can also be expressed in terms of these angles; i.e.

$$g_{sww}^{or}(\omega, \omega') = g_{sw}^{or}(\omega) g_{sw}^{or}(\omega') g_{ww}^{or,inh}(\omega, \omega') \quad (45)$$

For the KSA^{or}, $g_{ww}^{or,inh}$ is equal to the bulk orientational water pair correlation function $g_{ww}^{or,o}$, which is naturally given in terms of relative water–water angles, $\omega^{rel} = (\theta_1, \theta_2, \phi, \chi_1, \chi_2)$ (see Figure 1b). The conversion from the first set of angles to the second can be achieved by delta function integration. For example,

$$g_{sww}^{or}(\theta_1, \theta_2) = \frac{1}{\Omega'} \int g_{sww}^{or}(\omega, \omega') \delta(\theta_1, \theta_2) d\omega d\omega' \quad (46)$$

where $\Omega' = \Omega^2 / \int \sin\theta_1 d\theta_1 \sin\theta_2 d\theta_2$, and $\delta(\theta_1, \theta_2)$ is a delta function. Similar equations hold for other marginal distributions, such as $g_{sww}^{or}(\theta_1, \theta_2)$, $g_{sww}^{or}(\chi_1, \chi_2)$, $g_{sww}^{or}(\theta_1, \chi_2)$, $g_{sww}^{or}(\chi_1, \theta_2)$, and $g_{sww}^{or}(\phi)$. They are calculated in the simulation as averages over certain ranges of \mathbf{r}_1 and \mathbf{r}_2 . We can test the validity of KSA^{or} (eq 30) by using $g_{ww}^{or,o}$ in eqs 45 and 46 and the known g_{sw}^{or} , performing the integrations in eq 46 and comparing the resulting distribution functions with the $g_{sww}^{or}(\theta_1, \theta_2)$ etc. obtained directly from the simulations. For this calculation we used the factorization approximation (see Methods) and the average over the first shell pure water marginal distributions for $g_{ww}^{or,o}$, as well as the average of g_{sw}^{or} over the first methane solvation shell.

In region S1S1 the g_{sww}^{or} marginal distributions obtained from the KSA^{or} (not shown) are slightly more structured than those from the simulation when r and s are similar (for example, $r = s = 3.7$ Å) and are less structured than those from the simulation when r and s are dissimilar (e.g., $r = 3.2$, $s = 5.0$, $t = 3.2$ Å). Thus, averaging over the region S1S1 tends to cancel out these discrepancies from the simulation results. In region S1S2, for configurations where the two molecules are collinear with the solute the g_{sww}^{or} distributions are more structured than the simulation results, but noncollinear configurations give g_{sww}^{or} that are less structured than the simulation results. Thus, again the average should be close to the simulation results. For region S2S2 orientational preferences are very weak (g_{sw} close to 1) and the g_{sww}^{or} from the simulation are very close to the pure solvent functions. Therefore, only slight deviations from KSA^{or} are expected in this region. Overall, these results suggest that although the KSA^{or} has significant errors, its use for the estimation of solvent reorganization energies and entropies should give meaningful values due to the averaging involved. In the following section, the KSA^{or} is therefore employed for this purpose.

C. Energy and Entropy from Correlation Functions. 1.

Solute–Solvent Energy and Entropy (E_{sw} and S_{sw}^{ord}). The solute–solvent energy can be calculated by eq 5, but it is easily obtained directly from the simulation. The solute–solvent

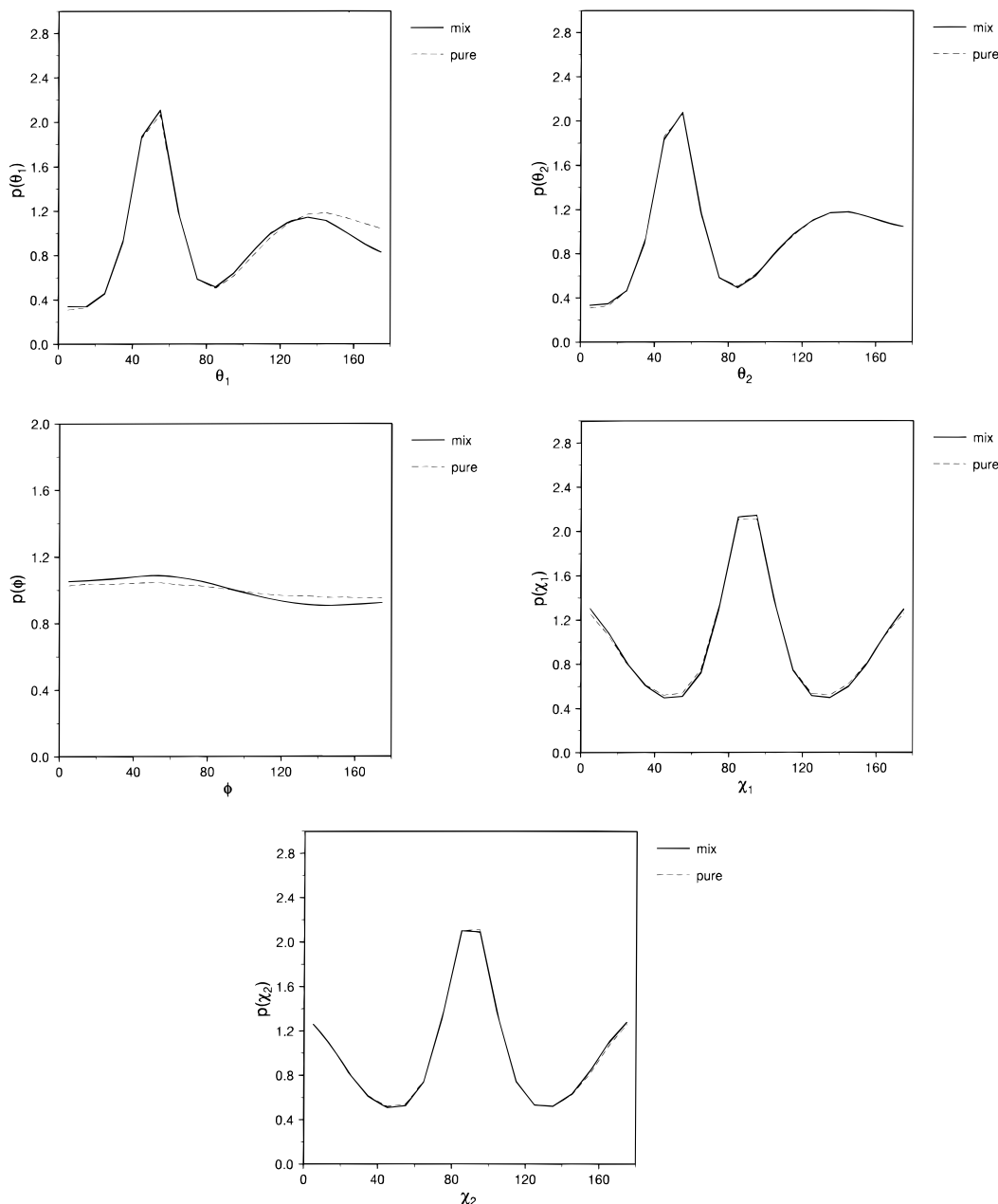


Figure 9. Water–water orientational correlations in region S1S2W1 at 25 °C: (a) $g(\theta_1)$; (b) $g(\theta_2)$; (c) $g(\phi)$; (d) $g(\chi_1)$; (e) $g(\chi_2)$.

entropy, $S_{\text{sw}}^{\text{ord}}$ (eq 6) has been calculated before.^{14,15} It can be split into a translational and an orientational part:³³

$$S_{\text{sw}}^{\text{ord,tr}} = -k\rho \int g_{\text{sw}}^{\text{r}} \ln g_{\text{sw}}^{\text{r}} \text{d}\mathbf{r} \quad (47)$$

$$S_{\text{sw}}^{\text{ord,or}} = -k\rho \int g_{\text{sw}}^{\text{r}} S(\mathbf{r}) \text{d}\mathbf{r} \quad (48)$$

with

$$S(\mathbf{r}) = \frac{1}{\Omega} \int g_{\text{sw}}^{\text{r}}(\omega|\mathbf{r}) \ln g_{\text{sw}}^{\text{or}}(\omega|\mathbf{r}) \text{d}\omega \quad (49)$$

The conditional orientational function $g_{\text{sw}}^{\text{or}}(\omega|\mathbf{r})$ was calculated for four regions of \mathbf{r} (see Methods). Thus, eq 48 becomes

$$S_{\text{sw}}^{\text{ord,or}} = -k \sum_{i=1}^4 S_i \rho \int_V g_{\text{sw}}^{\text{r}} \text{d}\mathbf{r} = -k \sum_{i=1}^4 S_i N_i \quad (50)$$

where N_i is the number of water molecules in region i .

The results for $S_{\text{sw}}^{\text{ord,tr}}$ and $S_{\text{sw}}^{\text{ord,or}}$ are shown in Table 2. The magnitude of both contributions decreases with increasing temperature, as expected. The magnitude of $S_{\text{sw}}^{\text{ord,or}}$ is larger than that of $S_{\text{sw}}^{\text{ord,tr}}$ at 25 °C but it decreases faster with temperature. This was also observed for the water–water correlations in pure water.³³

2. Solvent Reorganization Energy and Entropy ($\Delta E_{\text{ww}}^{\text{cor}}$ and $\Delta S_{\text{ww}}^{\text{cor}}$). To obtain $\Delta E_{\text{ww}}^{\text{cor}}$ and $\Delta S_{\text{ww}}^{\text{cor}}$, the orientationally averaged energy and orientational entropy U^{m} and S^{m} (eqs 15 and 21) were calculated at a grid of points r, s, t . The results for U^{m} and S^{m} for $r = 3.571 \text{ \AA}$ and $t = 2.857 \text{ \AA}$ as a function of s are shown in Figure 11. The value of s around 3.571 \AA corresponds to a configuration in S1S1W1, where both water molecules are in the first solvation shell of the solute (Figure 2). At this point, U^{m} and S^{m} are larger in magnitude than their pure solvent equivalents U^{o} and S^{o} . The same is true for s around 6.25 \AA , which corresponds to a collinear arrangement of the three

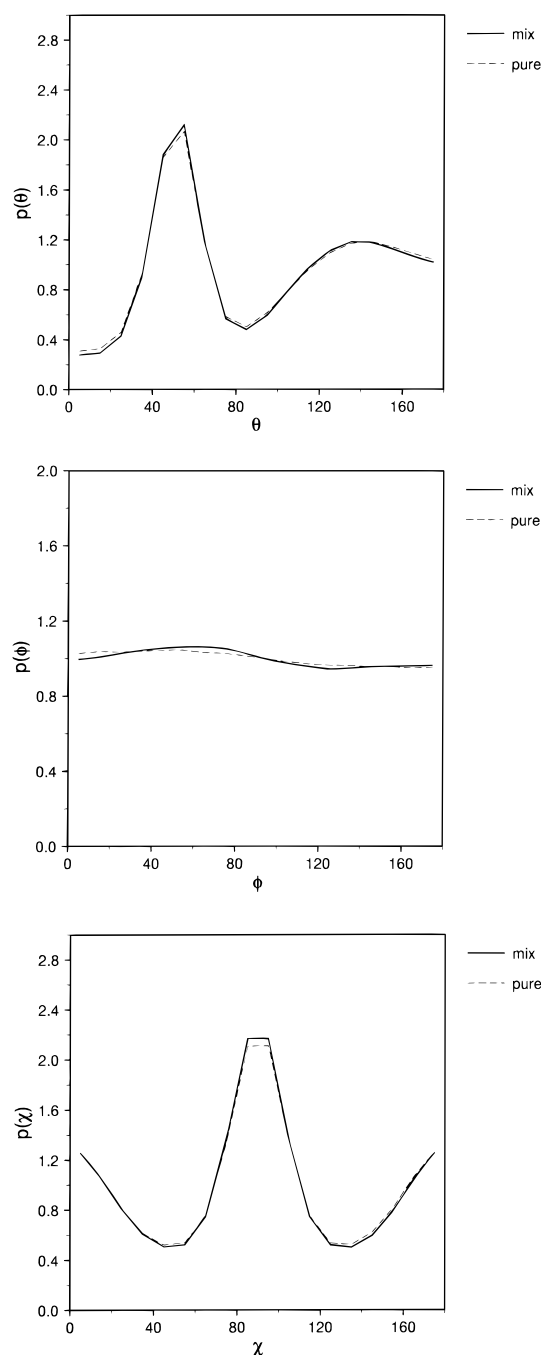


Figure 10. Water–water orientational correlations in region S2S2W1 (both in second solvation shell) at 25 °C: (a) $g(\theta)$; (b) $g(\phi)$; (c) $g(\chi)$.

molecules. At intermediate values of s the magnitude of U^m and S^m is smaller than U^o, S^o . This results from the fact that the orientational preferences for the two molecules with respect to the solute in this configuration are not conducive to good hydrogen bonding between them.

Integration over r, s, t gives the results shown in Table 3 for FAC and AGP; see section IIID for definitions. The results are obtained using KSA^{or} and the radial distribution correction δg_3 (eq 43) from the simulation. The excluded volume contribution is the total contribution from regions with $is = 0$ (s between 0 and 2.7 Å), as defined in section IIID. The largest contribution to the excluded volume term comes from the (101) region. The physical origin of this positive contribution is that the solute excludes solvent molecules from the region it occupies so that first solvation shell solvent molecules have fewer solvent

TABLE 2: Summary of Results from the Correlation Functions^a

	25 °C	65 °C	160 °C
$S_{sw}^{ord, tr}$	-7.43	-5.39	-2.86
$S_{sw}^{ord, or}$	-8.29	-4.85	-1.55
E_{sw}	-2.945	-2.679	-2.183
ΔS_{ww}^{trans}	-6.04	-1.75	0.36
ΔS_{ww}^{trans} (2-particle) ^b	-3.79	0.01	4.24

	FAC	AGP	FAC	AGP	FAC	AGP
ΔS_{ww}^{or}	-3.16	-2.05	-0.87	0.09	3.44	4.97
ΔE_{ww}	2.28	5.37	2.68	6.07	5.34	9.67

^a Energies in kcal/mol, entropies in cal/mol K. ^b Corresponding to the two-particle contribution in the homogeneous view (obtained using $\ln g_{ww}^o$ instead of $\ln g_{ww}^{inh}$ in eq 8).

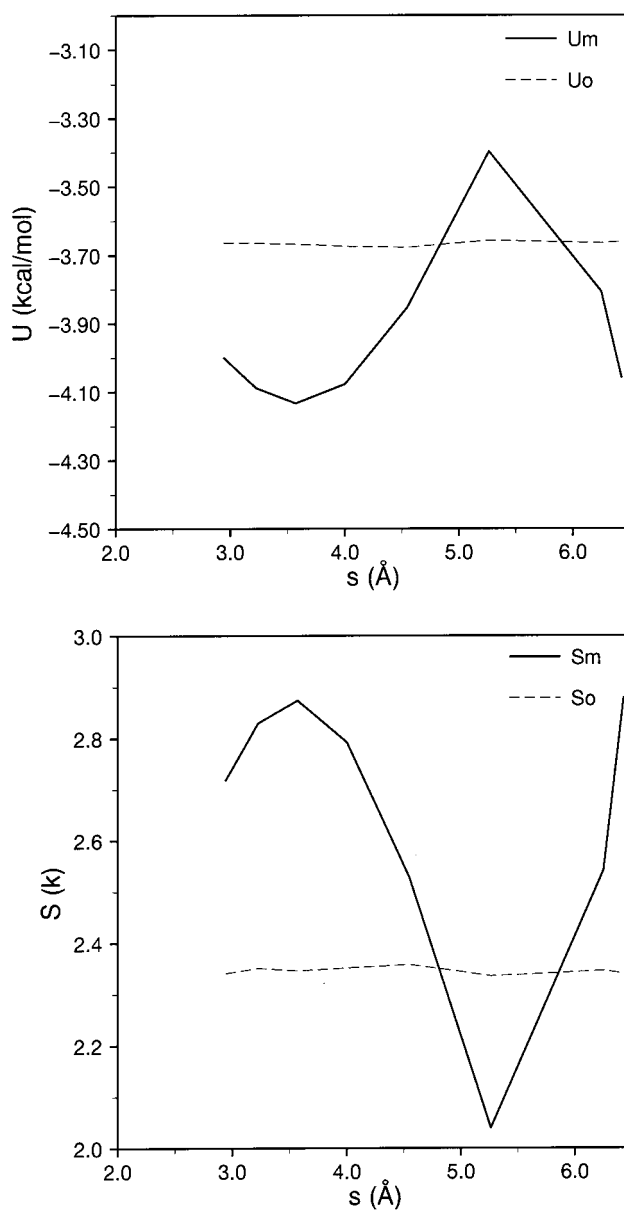


Figure 11. Orientationally averaged energy (a) and entropy (b) in the mixture (solid line) as a function of s for $r = 3.571$ Å and $t = 2.857$ Å at 65 °C. Dashed lines are the bulk values.

neighbors. This large positive contribution is more than compensated by a negative contribution from region (111) (all three molecules first neighbors of each other). Smaller but significant positive contributions come from regions (121),

TABLE 3: Solvent Reorganization Energy (kcal/mol) and Entropy (k) at 25 °C^a

<i>ir</i>	<i>is</i>	<i>it</i>	ΔS_{ww}^{tr}	FAC		AGP	
				ΔS_{ww}^{or}	ΔE_{ww}	ΔS_{ww}^{or}	ΔE_{ww}
1	1	1	-5.05	-14.96	-19.74	-16.90	-22.72
1	2	1	.66	2.58	4.50	3.04	5.79
1	0	1	2.57	9.81	14.65	11.47	18.38
1	0	2	.05	.48	2.04	.58	1.57
2	2	1	.24	1.49	2.05	1.74	2.49
totals			-3.04	-1.59	2.28	-1.03	5.37

^a Only regions with contributions greater than 1 kcal/mol or 1 k are shown.

TABLE 4: Solvent Reorganization Energy (kT) and Entropy (k) in LJ Fluid ($\rho^* = 0.85$, $T^* = 0.88$)^a

<i>ir</i>	<i>is</i>	<i>it</i>	ΔS_{ww}^{tr}	ΔE_{ww}
1	1	1	-3.49	-3.58
1	2	1	1.15	.49
1	4	1	4.38	6.13
2	1	1	-2.78	-6.50
2	1	2	-0.49	-2.21
2	2	1	1.01	2.07
2	4	1	1.02	3.32
2	4	2	.63	2.99
3	1	2	-0.27	-1.29
3	1	3	-0.27	-1.20
3	4	3	.27	1.19
totals			2.32	4.86

^a Only regions with contributions greater than 1 kcal/mol or 1 k are shown.

(221), and (102). These results are obtained with both the FAC and the AGP approximations.

For comparison, the contributions to the solvent reorganization energy and entropy for a LJ fluid ($\rho^* = \rho\sigma^3 = 0.85$, $T^* = kT/\epsilon = 0.88$, solute identical to solvent)³⁵ are shown in Table 4. As in water, the largest positive contribution comes from region (101) but it is smaller in magnitude. Region (111) makes a negative contribution, but its magnitude is much smaller than in water. Significant negative contributions come from regions (211), (212), (312), (313).

The total values for methane in water at 25 °C are -3.04 k for ΔS_{ww}^{tr} , -1.59 k (FAC) or -1.03 k (AGP) for ΔS_{ww}^{or} and 2.28 kcal/mol (FAC) or 5.37 kcal/mol (AGP) for ΔE_{ww} . If KSA^{tr} is employed ($\delta g_3 = 1$), the values for all quantities are significantly more positive: $\Delta S_{ww}^{tr} = 1.48$ k, $\Delta S_{ww}^{or} = 3.46$ k (FAC) or 3.973 k (AGP) and $\Delta E_{ww} = 7.16$ kcal/mol (FAC) or 10.63 kcal/mol (AGP). This is so because the deviations from KSA^{tr} enhance the probability of configurations that lead to attractive interactions and correlations between the first shell water molecules.

As explained in ref 34, eq 8 for ΔS_{ww} includes the homogeneous three-particle solute-solvent-solvent term $\int g^{(3)} \ln \delta g_3$. To make the results correspond to the homogeneous two-particle ΔS_{ww} term (the change in $\int \{g_{ww} \ln g_{ww} - g_{ww} + 1\} dr$) upon solute insertion, where g_{ww} is the homogeneous water pair correlation function), we need to replace $\ln g_{ww}^{inh}$ in eq 8 by $\ln g_{ww}^o$ leaving everything else the same, which leads to replacing $\ln g_{ww}^{r,inh}$ by $\ln g_{ww}^{r,o}$ in eq 23. That would give a translational entropy change $\Delta S_{ww}^{trans} = -1.91$ k.

The explicit use of solute-solvent and solvent-solvent correlation functions allows us to isolate the effect of particular correlation functions on the results and answer “what if” types of questions. One can compare, for example, the results obtained with the calculated value of g_{sw}^{or} , which deviates from unity

TABLE 5: Solvent Reorganization Energy (kcal/mol) and Entropy (k) at 65 °C^a

<i>ir</i>	<i>is</i>	<i>it</i>	ΔS_{ww}^{tr}	FAC		AGP	
				ΔS_{ww}^{or}	ΔE_{ww}	ΔS_{ww}^{or}	ΔE_{ww}
1	1	1	-3.51	-10.67	-14.79	-11.91	-17.04
1	2	1	.42	1.04	2.08	1.22	2.81
1	0	1	2.33	8.29	13.09	9.65	16.97
1	0	2	.01	.41	1.78	.55	1.78
2	1	1	.14	-1.29	-1.64	-1.51	-2.05
2	2	1	.43	1.72	2.35	1.87	2.73
totals			-0.88	-0.43	2.68	0.05	6.07

^a Only regions with contributions greater than 1 kcal/mol or 1 k are shown.

because water orients itself next to a hydrophobic solute, with the results for $g_{sw}^{or} = 1$, corresponding to no orientational preferences. With $g_{sw}^{or} = 1$ and the KSA^{or}, $U^m = U^o$ and $S^m = S^o$ everywhere and the results are $\Delta E_{ww} = 8.84$ (FAC) or 11.65 kcal/mol (AGP) and $\Delta S_{ww}^{or} = 4.06$ (FAC) or 5.83 k (AGP); that is, both ΔE_{ww} and ΔS_{ww}^{or} are significantly more positive. The energy and entropy changes can be combined to give the free energy change for the “structural relaxation” of water around a hydrophobic solute, i.e., the change from $g_{sw}^{or} = 1$ to the true g_{sw}^{or} . Using the FAC values, the difference in ΔE_{ww} is $8.84 - 2.28 = 6.6$ kcal/mol and the difference in ΔS_{ww} is $4.06 - (-1.59) = 5.65$ k from the water-water entropy and 4.17 k from the solute-water entropy, so that the total entropy difference is 9.82 k, which corresponds to 5.85 kcal/mol at 25 °C. Thus, the energy and entropy changes from the structural relaxation of water largely compensate and the net favorable free energy change is only -0.75 kcal/mol. With the AGP values, the corresponding free energy change is slightly unfavorable (0.25 kcal/mol). Clearly, this small free energy difference is within the uncertainty of the calculations. Physically, the free energy of this hypothetical process must be negative, since this structural relaxation is spontaneous. The calculations show that, due to partial energy-entropy compensation, the magnitude of the free energy change due to water relaxation around a hydrophobic solute is much smaller than the magnitudes of the separate energy and entropy changes. Moreover, it is evident that the energy-entropy balance in the free energy crucially depends on g_{sw}^{or} , the orientational distribution of water with respect to the solute.

The results at 65 °C are shown in Table 5. In comparison to 25 °C, ΔS_{ww}^{trans} is substantially less negative (-0.88 k versus -3.04 k at 25 °C). This is primarily due to the reduction in structure of δg_3 at the higher temperature; if the 25 °C values of δg_3 are used in eqs 23 and 44 and the other quantities are taken from the 65 °C results, the value is -2.22 k. The excluded volume contribution (101 etc., entries in Table 5) decreases because the pure solvent energy and entropy decrease in magnitude. The orientational arrangement contribution (111) decreases in magnitude as well. This is due primarily to the flattening of g_{sw}^{or} and secondarily to changes in δg_3 (if the 25 °C δg_3 is used, the 111 contribution to ΔE_{ww} becomes -16.07 for FAC and -18.35 kcal/mol for AGP). The calculated ΔE_{ww} at 65 °C is somewhat more positive than at 25 °C (2.68 versus 2.28 kcal/mol for FAC and 6.07 versus 5.37 kcal/mol for AGP).

The value of ΔC_p estimated from this change in ΔE_{ww} with temperature (5 k (FAC) or 8.7 k (AGP)) is much smaller than that calculated from the ΔE_{ww} values obtained directly from the simulation (see Table 1 and section IVA). This may be due to the use of the KSA^{or} or to the other approximations employed in these calculations (i.e., the approximations for g_{ww} and the

TABLE 6: Average Pair Energies (kcal/mol) and Entropies (k) at 25 °C

		FAC	AGP	simulation
S1S1W1	Ener	-3.164	-3.872	-3.63
	Entr	2.232	2.564	
S1S2W1	Ener	-2.782	-3.483	-3.17
	Entr	1.905	2.215	
S2S2W1	Ener	-2.835	-3.542	-3.23
	Entr	1.945	2.251	
BULK W1	Ener	-2.819	-3.554	-3.09
	Entr	1.882	2.251	

TABLE 7: Experimental Data^{a,b}

	25 °C	65 °C	160 °C
ΔG^*	1.994	2.512	4.16
ΔH^*	-2.605	-0.544	2.70
ΔS^*	-15.435	-9.02	-3.37
ΔC_p	56.6 (50 °C)		

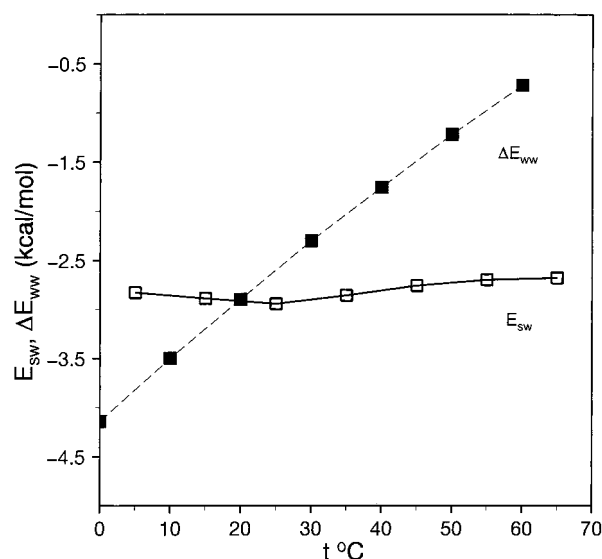
^a Energies in kcal/mol, entropies and heat capacities in cal/mol K.

^b Reference 55. Results at 65 and 160 °C from extrapolation using the experimental ΔC_p and $d\Delta C_p/dT$. Change of standard states was performed according to Ben-Naim and Marcus.³⁸ The extrapolation is probably not very reliable at 160 °C. ^c Reference 56.

interpolation schemes for g_{sw}^o , g_{sw}^m , or U^m and S^m , see sections IIIB, C, D). At 160 °C, the contributions to ΔE_{ww} and ΔS_{ww} (not shown) are qualitatively similar to those at 65 °C.

A more stringent test of the quality of the approximate correlation functions (i.e., g_{ww}^{inh} and g_{ww}^o) can be made by calculating the average interaction energies of first neighbor water molecules and comparing them to those obtained directly from the simulation. The calculated average water pair energies in regions S1S1W1, S1S2W1, S2S2W1 are given in Table 6. Both approximations show an enhanced water–water interaction in region S1S1W1 relative to the bulk. However, the percent increase from the bulk value is not as large as the simulation results (12% for FAC and 9% for AGP, vs 17% from the simulation). In regions S1S2W1 and S2S2W1 the average pair energies come out very close to the bulk values or even a little smaller in magnitude (for S1S2W1), whereas a slight enhancement is seen in the simulation results. These deviations may be due to either KSA^{or} or the interpolation scheme for g_{sw}^{or} . It can be seen that the magnitudes of the FAC values are underestimates and the AGP values are overestimates; in fact, the averages of the two are close to the simulation results. This is likely to be true for the pair entropies, as well, although no direct calculation of these quantities is possible to test this possibility. The results for the various components of the solvation energy and entropy obtained from the correlation functions are summarized in Table 2.

3. Comparison with Experimental Solvation Data. The experimental thermodynamic properties of solvation for methane in water are shown in Table 7. The enthalpy of solvation at 25 °C is -2.605 kcal/mol. The $P\Delta V^*$ contribution to it is negligible (less than 1 cal/mol), so that $\Delta H^* \approx \Delta E^* = E_{sw} + \Delta E_{ww}$. If we estimate ΔE_{ww} as the difference between the experimental ΔH^* and the (reliably) computed E_{sw} , we obtain Figure 12. E_{sw} does not vary much with temperature. At room temperature, E_{sw} is close to ΔH^* itself, therefore ΔE_{ww} is expected to be close to zero. ΔE_{ww} is expected to be negative below room temperature and to become increasingly positive with increasing temperature above 300 K. The values for ΔE_{ww} obtained directly from simulation (see Table 1) or from the approximate correlation functions (Table 5) are consistent with these ideas, although not sufficiently accurate for quantitative comparisons.

**Figure 12.** Solute–solvent interaction from the simulations (solid line/empty squares) and solvent reorganization energy obtained by difference from the experimental data as a function of temperature (dashed line/solid squares).

A similar pattern is observed for the entropy. The solute–solvent entropy at 25 °C ($S_{sw}^{ord} = -15.73$ e.u.) is very close to the experimental ΔS^* , which suggests that the remaining contributions to the entropy (ΔS_{ww} and higher order terms such as those related to the triplet water–water–water correlation function) largely cancel out. The value of S_{sw}^{ord} is a satisfactory approximation to ΔS^* at the other temperatures as well.

In comparing theoretical results with experimental data, it is important to separate the effects of the potential energy functions from the effects of the approximations involved in the calculation of the solvation energy and entropy. The potentials used in this work for methane have given good values for the solvation free energy.²⁴ The solvation energy and entropy for methane in SPC water were calculated by Guillot et al.²⁵ using the particle insertion method. They obtained -21.3 cal/mol K for the entropy and -3.9 kcal/mol for the energy. It should be noted that these values are for solute insertion at constant volume, which are more negative than the constant pressure solvation properties by 5 cal/mol K (entropy) and 1.5 kcal/mol (energy).⁶⁰ Taking this into account, the results for SPC are in good agreement with experiment. One can expect similar performance for TIP4P water.

The calculated solute–solvent energy and entropy are highly accurate and do not involve drastic approximations. They are, therefore, reliable. In contrast, the solvent reorganization energy and entropy result from cancellation of large contributions and depend sensitively on the molecular water–water correlation function, for which only approximations are available. As a result, the calculation of these quantities is not of sufficient accuracy at present to make quantitative comparison with experiment. However, the present calculations are important for a qualitative understanding of the physical origin of solvation thermodynamics.

V. Discussion

In this paper, estimates of the solvent reorganization energy and entropy for methane in water were made based on approximate calculations of the correlation functions involved. Although the definition of the solvent reorganization energy is clear, the definition of the solvent reorganization entropy is not.

For example, some authors identify it with the total solvation entropy.⁶¹ The definition adopted here is based on analogy with the decomposition of the energy (see eqs 5–8). The solute–solvent terms depend only on the solute–solvent correlation function. The solvent reorganization terms are due to the change in the solvent–solvent correlation function upon solute insertion.

The solvent reorganization energies can be calculated directly from the simulation, either by the difference of the water–water energy of by integration of the difference in binding energy from the bulk value, the latter method being more precise. It was found that for TIP4P water the binding energy in the first shell is similar to the bulk at room temperature and higher than the bulk at higher temperatures. First shell water molecules have fewer water neighbors but spend more time interacting favorably with them so that their average binding energy at room temperature is about the same as in the bulk.

Unlike the energy, the solvent reorganization entropy can only be calculated by explicit integration over water–water correlation functions in the mixture and in the pure solvent. Because these correlation functions are too complex to calculate directly by simulations, simplifying approximations for the orientational part must be employed. These approximations, as well as the inherent statistical uncertainty in the simulations, limit the quantitative accuracy of the resulting values. However, several qualitative conclusions can be clearly drawn. First, the small values of the solvent reorganization energy and entropy result from cancellation of two large contributions: the positive excluded volume contribution and the negative contribution from the orientational arrangement of water molecules in the first solvation shell (see section IVC2). These contributions are much larger than in a Lennard-Jones fluid. Second, as temperature increases, the solvent reorganization properties increase significantly, mainly due to flattening of the orientational distribution of water with respect to the solute.

The entropy of solvation of nonpolar gases in water increases with temperature, reaches zero at some point between 150 and 170 °C, and becomes positive at higher temperatures.⁶² Based on the present decomposition of the entropy into solute–solvent and solvent reorganization terms and the results at 25, 65, and 160 °C, the temperature dependence of ΔS can be explained as follows. At room-temperature S_{sw} is large and negative and ΔS_{ww} is close to zero. As temperature increases, S_{sw} diminishes in magnitude and ΔS_{ww} increases (becomes more positive). At some temperature there will be cancellation between the negative S_{sw} and the positive ΔS_{ww} , and beyond this temperature the positive ΔS_{ww} will dominate. This does not mean that at the crossing temperature the structure characteristic of hydrophobic hydration does not exist or that “hydration vanishes”. The simulations at 160 °C show that the structure around methane is still that characteristic of hydrophobic hydration, only the orientational preferences are much weaker than at room temperature. It is noted that the excess partial molar entropy of methane in a water-like LJ fluid (LJWAT in ref 35) is positive due to dominance of the ΔS_{ww} term. Thus, it could be argued that LJWAT resembles high-temperature water in this respect.

The results presented herein confirm the conclusions of previous work that the major contribution to the entropy of hydrophobic hydration at room-temperature comes from solute–solvent correlations, primarily within the first solvation shell,^{63,14,15,32} rather than from changes in solvent–solvent correlations. The situation is similar to that for the solvation energy. The solvation energy at room temperature is well accounted for by the solute–solvent interaction alone.^{20,19} The solvent reorganization energy is small because water molecules

next to the solute manage to maintain their hydrogen bonds by adopting preferential orientations with respect to it. At higher temperatures entropy weighs more heavily in the free energy ($\Delta G = \Delta H - T\Delta S$) and the system prefers to maximize the entropy rather than minimize the energy. Thus, as the temperature increases, the orientational structure is destroyed, leading to increasing loss of hydrogen bonding between solvent molecules and an increase in the solvation energy.

From the results of this work, the large and positive value of ΔC_p is due to the sharp increase in solvent reorganization energy with temperature. The fundamental structural parameter that determines the entropy–energy balance is g_{sw}^{or} . At higher temperature entropy becomes more important, g_{sw}^{or} becomes flatter, δg_3 structure diminishes, S_{sw} and ΔS_{ww} increase, and ΔE_{ww} increases because of increasing loss of water–water hydrogen bonds. This is in agreement with simple thermodynamic models based on water orientations next to a solute.^{64,65} Sometimes, the fact that the solvation heat capacity is positive is taken as indication of structure promotion. This is not justified. ΔC_p shows the extent to which structure in the mixture can be broken with an increase in temperature. This can be large even if the solvent structure is already “broken” compared to the bulk. Thus, a positive ΔC_p can be observed with both structure making and breaking. That is why ΔC_p can be high at high temperatures even though water structure is definitely broken at those temperatures compared to pure water.⁶⁶

These conclusions on the heat capacity differ somewhat from a study based on the random network model of water.⁵⁸ In that work, the solvent reorganization term was indeed found to make the major contribution to ΔC_p , but it was smaller than one would expect based on the experimental ΔC_p values (the total calculated ΔC_p was significantly smaller than the experimental value). This underestimation may have been due to the fact that the temperature derivatives of the random network model parameters (average and RMS of oxygen–oxygen distance and RMS of hydrogen bonding angle) next to the solute are likely to be larger than in the bulk. Physically, that work suggested that the large heat capacity is due to a shortening of the OO distance and narrowing of the RMS angle fluctuations (essentially water–water structure making). However, this cannot explain the fact that the heat capacity is also large at high temperatures, where such narrowing is not expected.

It has been argued that the specific structural relaxation of water around a nonpolar solute actually decreases its solvation free energy,^{67,68} rather than being the “cause” of the low solubility of hydrophobic molecules in water. The present results are consistent with this view. Obviously, by adopting a clathrate-like arrangement around small nonpolar solutes water molecules avoid the very costly loss of hydrogen bonds. The calculations show explicitly that the energy and entropy changes are very large for water structural relaxation but they largely compensate to produce a very small free energy change. In contrast, the process of solute insertion produces a significant net free energy change. These observations are in agreement with arguments made by Lee.⁶⁹

A popular thermodynamic model for hydrophobic hydration is the one proposed by Muller.⁶⁶ The model assumes an increased enthalpy and entropy for breaking of hydrogen bonds in the hydration shell than in the bulk and obtains the fraction of broken hydrogen bonds from an equilibrium-type treatment of hydrogen bond formation. The major deficiency of this model is the neglect of solute–solvent energy and entropy. All solvation properties are assumed to arise from changes in solvent–solvent hydrogen bonding. Second, the assumption that

the energy and entropy of hydrogen bond breaking is higher in the hydration shell is a rather ad hoc assumption and does not exactly correspond to reality. It is physically more reasonable to distinguish hydration shell and bulk water through the temperature derivative of the fraction of broken hydrogen bonds. In the hydration shell, hydrogen bonds are more susceptible due to geometric factors (the solute excluded volume). Indeed, a simple two-dimensional model of water showed that the fraction of broken hydrogen bonds increases with temperature faster in the hydration shell than in the bulk.⁶¹ Such factors are not included in Muller's model.

One issue that is still being debated is the origin of hydrophobicity, i.e., which molecular property of water is primarily responsible for the positive solvation free energy of nonpolar groups and their tendency to associate. The two main propositions are (a) the large cohesive energy density of water (the fact that, due to hydrogen bonds, water–water interactions are very strong whereas nonpolar–water interactions are weak),^{70–72,68} and (b) the small size of water.^{73,74} The results presented herein are consistent with the former view. A more detailed analysis of this issue will be presented in a future publication.

Acknowledgment. This work was carried out at the Department of Chemistry at Harvard University where the author was a Burroughs Wellcome PMMB Postdoctoral fellow. Extensive comments and suggestions by Prof. Martin Karplus are gratefully acknowledged. Partial support has also been provided by a RCMI grant to CCNY from the National Institutes of Health.

References and Notes

- Pratt, L. R.; Chandler, D. *J. Chem. Phys.* **1977**, *67*, 3683.
- Ichiye, T.; Chandler, D. *J. Phys. Chem.* **1988**, *92*, 5257.
- Yu, H.-A.; Roux, B.; Karplus, M. *J. Chem. Phys.* **1990**, *92*, 5020.
- Yu, H.-A.; Pettitt, B. M.; Karplus, M. *J. Am. Chem. Soc.* **1991**, *113*, 2425.
- Hummer, G.; Garde, S.; Garcia, A. E.; Pohorille, A.; Pratt, L. R. *Proc. Natl. Acad. Sci. U.S.A.* **1996**, *93*, 8951.
- Hummer, G.; Garde, S.; Garcia, A. E.; Paulaitis, M. E.; Pratt, L. R. *J. Phys. Chem. B* **1998**, *102*, 10469.
- Owicki, J. C.; Scheraga, H. A. *J. Am. Chem. Soc.* **1977**, *99*, 7413.
- Swaminathan, S.; Harrison, S. W.; Beveridge, D. L. *J. Am. Chem. Soc.* **1978**, *100*, 5705.
- Geiger, A.; Rahman, A.; Stillinger, F. H. *J. Chem. Phys.* **1979**, *70*, 263.
- Pangali, C.; Rao, M.; Berne, B. J. *J. Chem. Phys.* **1979**, *71*, 2982.
- Rosky, P. J.; Karplus, M. *J. Am. Chem. Soc.* **1979**, *101*, 1913.
- Alagona, G.; Tani, A. *J. Chem. Phys.* **1980**, *72*, 580.
- Postma, J. P. M.; Berendsen, H. J. C.; Haak, J. R. *Faraday Symp. Chem. Soc.* **1982**, *17*, 55.
- Lazaridis, T.; Paulaitis, M. E. *J. Phys. Chem.* **1992**, *96*, 3847.
- Lazaridis, T.; Paulaitis, M. E. *J. Phys. Chem.* **1994**, *98*, 635.
- Vaisman, I. I.; Brown, F. K.; Tropsha, A. *J. Phys. Chem.* **1994**, *98*, 5559.
- Meng, E. C.; Kollman, P. A. *J. Phys. Chem.* **1996**, *100*, 11460.
- Zichi, D. A.; Rosky, P. J. *J. Chem. Phys.* **1985**, *83*, 797.
- Durell, S. R.; Wallqvist, A. *Biophys. J.* **1996**, *71*, 1695.
- Jorgensen, W. L.; Gao, J.; Ravimohan, C. *J. Phys. Chem.* **1985**, *89*, 3470.
- Yu, H.-A.; Karplus, M. *J. Chem. Phys.* **1988**, *89*, 2366.
- Lee, B. *Biopolymers* **1991**, *31*, 993.
- Straatsma, T. P.; Berendsen, H. J. C.; Postma, J. P. M. *J. Chem. Phys.* **1986**, *85*, 6720.
- Jorgensen, W. L.; Blake, J. F.; Buckner, J. K. *J. Chem. Phys.* **1989**, *129*, 193.
- Guillot, B.; Guissani, Y.; Bratos, S. *J. Chem. Phys.* **1991**, *95*, 3643.
- Radmer, R. J.; Kollman, P. A. *J. Comput. Chem.* **1997**, *18*, 902.
- Daura, X.; Mark, A. E.; Gunsteren, W. F. v. *J. Comput. Chem.* **1998**, *19*, 535.
- Guillot, B.; Guissani, Y. *J. Chem. Phys.* **1993**, *99*, 8875.
- Smith, D. E.; Haymet, A. D. J. *J. Chem. Phys.* **1993**, *98*, 6445.
- Wallace, D. C. *J. Chem. Phys.* **1987**, *87*, 2282.
- Baranyai, A.; Evans, D. J. *Phys. Rev. A* **1989**, *40*, 3817.
- Ashbaugh, H. S.; Paulaitis, M. E. *J. Phys. Chem.* **1996**, *100*, 1900.
- Lazaridis, T.; Karplus, M. *J. Chem. Phys.* **1996**, *105*, 4294.
- Lazaridis, T. *J. Phys. Chem.* **1998**, *102*, 3531.
- Lazaridis, T. *J. Phys. Chem.* **1998**, *102*, 3542.
- Percus, J. K. In *The equilibrium theory of classical fluids*; Frisch, H. L.; Lebowitz, J. L., Eds.; Benjamin: New York, 1964; pp 113–170.
- Ben-Naim, A. *J. Phys. Chem.* **1978**, *82*, 792.
- Ben-Naim, A.; Marcus, Y. *J. Chem. Phys.* **1984**, *81*, 2016.
- Matubayasi, N.; Reed, L. H.; Levy, R. M. *J. Phys. Chem.* **1994**, *98*, 10640.
- CRC Handbook of Chemistry and Physics*; 64th ed.; Weast, R. C., Ed.; CRC Press: Boca Raton, 1983–84.
- Masterton, W. L. *J. Chem. Phys.* **1954**, *22*, 1830.
- Jorgensen, W. L. BOSS, version 2.8; Yale University: New Haven, CT, 1989.
- Jorgensen, W. L.; Chandrasekhar, J.; Madura, J. D.; Impey, R. W.; Klein, M. L. *J. Chem. Phys.* **1983**, *79*, 926.
- Jorgensen, W. L.; Madura, J. D.; Swenson, C. J. *J. Am. Chem. Soc.* **1984**, *106*, 6638.
- Krumhansl, J. A.; Wang, S.-S. *J. Chem. Phys.* **1972**, *56*, 2034.
- Press, W. H.; Flannery, B. P.; Teukolsky, S. A.; Vetterling, W. T. *Numerical Recipes, Fortran version*; Cambridge University Press: Cambridge, 1989.
- Berntsen, J.; Espelid, T. O.; Genz, A. *Trans. Math. Soft.* **1991**, *17*, 452.
- Conroy, H. J. *J. Chem. Phys.* **1967**, *47*, 5307.
- Sloan, I. H.; Joe, S. *Lattice methods for multiple integration*; Clarendon: Oxford, 1994.
- Kusalik, P. G.; Lider, F.; Svishchev, I. M. *J. Chem. Phys.* **1995**, *103*, 10169.
- Levy, R. M.; Gallicchio, E. *Annu. Rev. Phys. Chem.* **1998**, *49*, 527.
- Head-Gordon, T.; Stillinger, F. H. *J. Phys. Chem.* **1993**, *98*, 3313.
- Stillinger, F. H.; Rahman, A. *J. Chem. Phys.* **1974**, *60*, 1545.
- Poole, P. H.; Sciortino, F.; Essmann, U.; Stanley, H. E. *Phys. Rev. E* **1993**, *48*, 3799.
- Rettich, T. R.; Handa, Y. P.; Battino, R.; Wilhelm, E. *J. Phys. Chem.* **1981**, *85*, 3230.
- Naghbi, H.; Dec, S. F.; Gill, S. J. *J. Phys. Chem.* **1986**, *90*, 4621.
- Bridgeman, C. H.; Buckingham, A. D.; Skipper, N. T. *Chem. Phys. Lett.* **1996**, *253*, 209.
- Madan, B.; Sharp, K. *J. Phys. Chem.* **1996**, *100*, 7713.
- de Jong, P. H. K.; Wilson, J. E.; Neilson, G. W.; Buckingham, A. D. *Mol. Phys.* **1997**, *91*, 99.
- Lazaridis, T.; Paulaitis, M. E. *J. Phys. Chem.* **1993**, *97*, 5789.
- Silverstein, K. A. T.; Haymet, A. D. J.; Dill, K. A. *J. Chem. Phys.* **1999**, *111*, 8000.
- Garde, S.; Hummer, G.; Garcia, A. E.; Paulaitis, M. E.; Pratt, L. R. *Phys. Rev. Lett.* **1996**, *77*, 4966.
- Rashin, A. A.; Bukatin, M. A. *J. Phys. Chem.* **1991**, *95*, 2942.
- Gill, S. J.; Wadso, I. *Proc. Natl. Acad. Sci. U.S.A.* **1976**, *73*, 2955.
- Gill, S. J.; Dec, S. F.; Olofsson, G.; Wadso, I. *J. Phys. Chem.* **1985**, *89*, 3758.
- Muller, N. *Acc. Chem. Res.* **1990**, *23*, 23.
- Shinoda, K. *J. Phys. Chem.* **1977**, *81*, 1300.
- Hvidt, A. *Annu. Rev. Biophys. Bioeng.* **1983**, *12*, 1.
- Lee, B. *Biophys. Chem.* **1994**, *51*, 271.
- Kauzmann, W. Denaturation of proteins and enzymes. In *The mechanism of enzyme action*; McElroy, W. D., Glass, B., Eds.; Johns Hopkins Press: Baltimore, 1954; p 71.
- Kirkwood, J. G. The nature of the forces between protein molecules in solution. In *The mechanism of enzyme action*; McElroy, W. D., Glass, B., Eds.; Johns Hopkins Press: Baltimore, 1954; p 16.
- Tanford, C. *The hydrophobic effect: Formation of micelles and biological membranes*, 2nd ed.; Wiley-Interscience: New York, 1980.
- Lucas, M. J. *J. Phys. Chem.* **1976**, *80*, 359.
- Lee, B. *Biopolymers* **1985**, *24*, 813.